Molecular Biology of the Cell
Vol. 17, 2524–2536, June 2006

Nuclear RanGAP Is Required for the Heterochromatin Assembly and Is Reciprocally Regulated by Histone H3 and Clr4 Histone Methyltransferase in *Schizosaccharomyces pombe*

Hitoshi Nishijima,*† Jun-ichi Nakayama,‡ Tomoko Yoshioka,* Ayumi Kusano,* Hideo Nishitani,* Kei-ichi Shibahara,† and Takeharu Nishimoto*

*Department of Molecular Biology, Graduate School of Medical Science, Kyushu University, Higashi-ku, Fukuoka 812-8582, Japan; †Department of Integrated Genetics, National Institute of Genetics, Mishima, Shizuoka 411-8540, Japan; and ‡Laboratory for Chromatin Dynamics, Center for Developmental Biology, RIKEN, Kobe 650-0047, Japan

Submitted September 26, 2005; Revised February 15, 2006; Accepted March 2, 2006
Monitoring Editor: Karsten Weis

Although the Ran GTPase-activating protein RanGAP mainly functions in the cytoplasm, several lines of evidence indicate a nuclear function of RanGAP. We found that *Schizosaccharomyces pombe* RanGAP, *Sp*Rna1, bound the core of histone H3 (H3) and enhanced Clr4-mediated H3-lysine 9 (K9) methylation. This enhancement was not observed for methylation of the H3-tail containing K9 and was independent of *Sp*Rna1–RanGAP activity, suggesting that *Sp*Rna1 itself enhances Clr4-mediated H3-K9 methylation via H3. Although most *Sp*Rna1 is in the cytoplasm, some cofractionated with H3. *Sprna1*^{ts} mutations caused decreases in Swi6 localization and H3-K9 methylation at all three heterochromatic regions of *S. pombe*. Thus, nuclear *Sp*Rna1 seems to be involved in heterochromatin assembly. All core histones bound *Sp*Rna1 and inhibited *Sp*Rna1–RanGAP activity. In contrast, Clr4 abolished the inhibitory effect of H3 on the RanGAP activity of *Sp*Rna1 but partially affected the other histones. *Sp*Rna1 formed a trimeric complex with H3 and Clr4, suggesting that nuclear *Sp*Rna1 is reciprocally regulated by histones, especially H3, and Clr4 on the chromatin to function for higher order chromatin assembly. We also found that *Sp*Rna1 formed a stable complex with Xpo1/Crm1 plus Ran-GTP, in the presence of H3.

INTRODUCTION

The concentration gradient of Ran-GTP from the nucleus to the cytoplasm (Kalab *et al*., 2002) is important to carry out the Ran-mediated cellular processes, such as nucleocytoplasmic transport of macromolecules, mitotic spindle formation, and postmitotic nuclear envelope assembly (Moore, 2001; Dasso, 2002; Hetzer *et al*., 2002; Weis, 2003; Mattaj, 2004). It is maintained by the cytoplasmic RanGAP (Becker *et al*., 1995; Bischoff *et al*., 1995a) and the chromosomal Ran-GDP/GTP exchange factor RCC1 (Kai *et al*., 1986; Ohtsubo *et al*., 1989; Bischoff and Ponstingl, 1991). Although RCC1 possesses only the nuclear localization signal (NLS) (Seino *et al*., 1992), RanGAP possesses a nuclear export signal (NES), in addition to NLS. For example, the *Saccharomyces cerevisiae* RanGAP homologue *Sc*Rna1p possesses a novel type of NLS and two of the classical NES signals, indicating that RanGAP is localized in the nucleus and exported, depending on the nuclear export receptor Xpo1/Crm1 (Feng *et al*., 1999). In *Drosophila melanogaster*, a naturally occurring meiotic drive system of the *Segregation Distorter* (*SD*) (Lyttle, 1991), which shows a preferential transmission of the *SD* chromosome from *SD/SD*$^+$ heterozygous males, is caused by a mutated RanGAP, referred to as Sd-RanGAP (Merrill *et al*., 1999). This is enzymatically active but lacks a functional NES, so Sd-RanGAP accumulates in the nucleus (Kusano *et al*., 2001). Yrb1p, an *S. cerevisiae* homologue of mammalian RanBP1 that enhances RanGAP activity (Bischoff *et al*., 1995b; Noguchi *et al*., 1997; Seewald *et al*., 2003), shuttles between the nucleus and cytoplasm (Kunzler *et al*., 2000). We have also found that disruption of the *S. cerevisiae YRB2* gene encoding a homologue of mammalian RanBP3, another RanGAP activator in the nucleus (Welch *et al*., 1999), is synthetically lethal with a temperature-sensitive mutant of *S. cerevisiae* RanGAP, *rna1-1* (Noguchi *et al*., 1997). These reports suggest a hitherto unsuspected role of RanGAP in the nucleus.

We previously isolated a series of the temperature-sensitive (ts) mutants of the *Sprna1*$^+$ gene encoding the *Schizosaccharomyces pombe* homologue of mammalian RanGAP. *Sprna1*^{ts} shows a defect in chromosome segregation rather than in mitotic spindle formation or nucleocytoplasmic transport (Kusano *et al*., 2004). Interestingly, the temperature sensitivity of *Sprna1*^{ts} is suppressed by overexpression of Clr4, a histone methyltransferase (HMTase) specific for histone H3 (H3)-K9 that is essential for heterochromatin assembly (Rea *et al*., 2000; Bannister *et al*., 2001; Nakayama *et al*., 2001), and is synthetically enhanced by a deletion of the *clr4*$^+$ gene. Consistently, *Sprna1*^{ts} shows a centromeric gene-silencing defect (Kusano *et al*., 2004). Thus, the phenotype of *Sprna1*^{ts} suggests that RanGAP might have an unsuspected nuclear function related to heterochromatin assembly. In this context, it is intriguing how RanGAP may be functionally related with Clr4-HMTase. Here, Clr4 and its substrate H3 were found to play an important role in regulating a nuclear RanGAP.

This article was published online ahead of print in *MBC in Press* (http://www.molbiolcell.org/cgi/doi/10.1091/mbc.E05–09–0893) on March 15, 2006.

Address correspondence to: Takeharu Nishimoto (tnishi@molbiol.med.kyushu-u.ac.jp).

Table 1. *S. pombe* strains used in this study

Strains[a]	Genotype
AK4	*h⁻ ura4-D18 leu1-32*
FY2267	*h⁺ ura4-D18 leu1-32 ade6-m210 clr4::ura4⁺ otr1R(dg-glu)Sph::ade6*
FY498	*h⁺ ura4-DS/E leu1-32 ade6-m210 imr1R(NcoI)::ura4⁺*
FY648	*h⁺ ura4-DS/E leu1-32 ade6-m210 otr1R(NcoI)::ura4⁺*
FY336	*h⁻ ura4-DS/E leu1-32 ade6-m210 cnt1/TM(NcoI)::ura4⁺*
HN1	*h⁻ ura4-D18 leu1-32* [pREP3X]
HN2	*h⁻ ura4-D18 leu1-32* [pREP3X-hht1]
HN3	*h⁻ ura4-D18 leu1-32* [pREP3X-NES-hht1]
HN4	*h⁺ ura4-D18 leu1-32 ade6-m210 clr4::ura4⁺ otr1R(dg-glu)Sph::ade6* [pREP3X]
HN5	*h⁺ ura4-D18 leu1-32 ade6-m210 clr4::ura4⁺ otr1R(dg-glu)Sph::ade6* [pREP3X-hht1]
HN6	*h⁺ ura4-D18 leu1-32 ade6-m210 clr4::ura4⁺ otr1R(dg-glu)Sph::ade6* [pREP3X-NES-hht1]
HN7	*h⁺ ura4-DS/E leu1-32 imr1R(NcoI)::ura4⁺*
HN8	*h⁻ ura4-DS/E leu1-32 imr1R(NcoI)::ura4⁺ sprna1-1ts*
HN9	*h⁻ ura4-DS/E imr1R(NcoI)::ura4⁺ sprna1-47ts*
HN10	*h⁻ ura4-DS/E leu1-32 imr1R(NcoI)::ura4⁺ sprna1-86ts*
HN11	*h⁺ ura4-DS/E leu1-32 imr1R(NcoI)::ura4⁺ sprna1-87ts*

[a] Strains FY498, FY648, and FY336 are described in Nakagawa *et al*. (2002). FY2267 is described in Bannister *et al.* (2001). Strains starting with AK are described in Kusano *et al*. (2004). Strains starting with HN are generated in this study.

MATERIALS AND METHODS

Yeast Media and Strains

S. pombe strains were grown in rich medium (YE5S) or Edinburgh minimal medium (EMM) with appropriate supplements. The strains used in this experiment are listed in Table 1.

Recombinant Protein Preparation

Clr4: *S. pombe clr4⁺* that was isolated previously (Kusano *et al*., 2004) was fused with 6xHis in-frame using pRSETc (Table 2) and was expressed in *Escherichia coli*. Clr4 was purified using Ni-NTA agarose (QIAGEN, Hilden, Germany) and MonoQ (GE Healthcare, Piscataway, NJ) as reported previously (Nakayama *et al*., 2001).

*Sp*Rna1: *S. pombe Sprna1⁺* and *Sprna1ts* genes were amplified from the *S. pombe* genomic DNA by PCR using as primers Rna1-N (5′-AAC GCG TCG ACA TGT CGC GTT TTT CAA TAG AAG GG) and Rna1-C (5′-AAA ACT GCA GCA TCC CTA AAT ATG AGC TTT TGA TAG CTC). Amplified DNA fragments were inserted into pQE31 (QIAGEN) (Table 2). Resulting 6xHis-fused *Sp*Rna1 was expressed in *E. coli* and purified using Ni-NTA agarose and MonoQ.

Hht1: *S. pombe hht1⁺* (*S. pombe* gene, no. SPAC1834.04), encoding a mammalian H3 homologue, was amplified from the *S. pombe* genomic DNA using as primers Hht1-N (5′-CCG CAT ATG GCT CGT ACT AAA CAA AC), Hht1-M (5′-CCG CAT ATG CGT TAT CGT CCT GGT ACT GT), Hht1-Ccom (5′-CGG GAT CCT TAT GAG CGT TCG CCA CGG A), and Hht1-Mcom (5′-CCG CAT ATG CGT TAT CGT CCT GGT ACT GT). Amplified DNA fragments were inserted into pET3b vectors (Table 2). A full-sized, core, and tail Hht1 were expressed in *E. coli* and purified as described previously (Luger *et al*., 1999). Purified proteins were conjugated to the beads, NHS-activated Sepharose 4FF (GE Healthcare), at 2 mg protein/ml Sepharose.

Analysis of Clr4-mediated HMTase Activity

Recombinant Clr4 (80 nM) was mixed with commercially available calf H3 (Roche Diagnostics, Mannheim, Germany) (8 μM), *S*-adenosyl-L-[methyl-^{14}C]methionine ([^{14}C]SAM) (80 μM) as the methyl donor, and the indicated proteins in 40 μl of HMTase buffer (50 mM Tris, pH 8.0, 20 mM KCl, 10 mM $MgCl_2$, 250 mM sucrose, and 0.5 mM dithiothreitol [DTT]). After incubation for 1 h at 30°C, each sample was given SDS sample buffer and boiled. Boiled samples were separated by 17% SDS-PAGE and visualized by Coomassie staining. ^{14}C-Labeled H3 was detected and analyzed using Bio-Imaging analyzer BAS-2500 (Fujifilm, Tokyo, Japan).

Methylation of the H3/Hht1-tail (ARTKQTARKSTGGKAPRKQL) and the Hht1-core was carried out in the same condition. After incubation with [^{14}C]SAM, the sample was spotted onto the P81 phosphocellulose filter paper (catalog no. 3698023; Whatman, Maidstone, United Kingdom) and washed four times by incubating each time for 10 min in 50 mM $NaHCO_3$, pH 9.0. The radioactivity incorporated into each substrate was calculated by liquid scintillation counter as described previously (Nakayama *et al*., 2001).

Analysis of RanGAP Activity

[γ-^{32}P]GTP was loaded on Ran by incubating for 10 min at 30°C in loading buffer (25 mM Tris, pH 7.5, 50 mM NaCl, 10 mM EDTA, and 1 mM DTT). The reaction was stopped with the addition of 20 mM $MgCl_2$ and the resulting Ran-[γ-^{32}P]GTP molecules were collected through a PD10 column (GE Healthcare) that had been equilibrated with GAP buffer (25 mM Tris, pH 7.5, 50 mM NaCl, 20 mM $MgCl_2$, 1 mM DTT, and 0.05% gelatin [catalog no. G-7765; Sigma-Aldrich, St. Louis, MO]). Fifty nanomolar Ran-[γ-^{32}P]GTP were incubated for 10 min at 30°C in 100 μl of GAP buffer containing various concentrations of *Sp*Rna1 and the indicated proteins. The reaction was stopped by addition of ice-cold stop buffer {20 mM Tris, pH 7.5, 25 mM $MgCl_2$, and 100 mM NaCl). Resulting reaction mixtures were spotted onto the nitrocellulose membrane (0.45 μm, NC45; Whatman Schleicher and Schuell, Dassel, Germany) and washed with ice-cold stop buffer. The radioactivity of the [γ-^{32}P]GTP remaining on Ran is calculated by a liquid scintillation counter.

To separate GTP and P_i, the reaction was stopped by the addition of EDTA (final concentration 72 mM), and the reaction mixtures were boiled. Samples (0.3 μl) were spotted on a thin layer chromatography plate (PEI matrix; Sigma-Aldrich) and then [γ-^{32}P]GTP and ^{32}P-labeled inorganic phosphate ($^{32}P_i$) were separated with 1 M LiCl and 1 M formic acid for 60 min. ^{32}P-labeled reagents were detected and analyzed using BAS-2500. By setting the

Table 2. Plasmids used in this study

Plasmid	Marker	Description	Reference
For yeast			
pREP3X	LEU2	Yeast-inducible expression vectors	Maundrell (1993)
pREP3X-hht1	LEU2	pREP3X with *hht1⁺* fragment at BamHI/SmaI site	This study
pREP3X-NES-hht	LEU2	pREP3X with *NES* fused *hht1⁺* fragment at XhoI/BamHI site	This study
For *E. coli*			
pRSETc-Clr4		pRSETc with *Clr4⁺* at BamHI/EcoRI site	Nakayama *et al.* (2001)
pQE31-Rna1		pQE31 with *Rna1⁺* at SalI/PstI site	This study
pQE31-Rna1-8		pQE31 with *Rna1-8ts* at SalI/PstI site	This study
pQE31-Rna1-15		pQE31 with *Rna1-15ts* at SalI/PstI site	This study
pQE31-Rna1-87		pQE31 with *Rna1-87ts* at SalI/PstI site	This study
pET3b-hht1FL		pET3b with *hht1⁺* (1-136) at NdeI/BamHI site	This study
pET3b-hht1N		pET3b with *hht1* (1-40) at NdeI/BamHI site	This study
pET3b-hht1C		pET3b with *hht1* (41-136) at NdeI/BamHI site	This study
pET8c-Ran		pET8c with Ran at NcoI/BamHI site	Dasso *et al*. (1994)
pET3b-RCC1		pET3b with RCC1 at NdeI/BamHI site	Dasso *et al*. (1994)
pGEX-CS-RanBP1		pGEX-CS with RanBP1 at NcoI/XhoI site	Hayashi *et al*. (1995)

Table 3. Primers used in ChIP assay

Locus	Name	Sequence	Reference
ura4	ura4FW	5′-GAGGGGATGAAAAATCCCAT-3′	Ekwall *et al.* (1997)
	ura4RV	5′-TTCGACAACAGGATTACGACC-3′	
act1	act1FW	5′-GAAGTACCCCATTGAGCACGG-3′	Noma *et al.* (2001)
	act1RV	5′-CAATTTCACGTTCGGCGGTAG-3′	
dg223	dg223FW	5′-TGGTAATACGTACTAGCTCTCG-3′	Nakagawa *et al.* (2002)
	dg223RV	5′-AACTAATTCATGGTGATTGATG-3′	
E12	B15E1-2490	5′-CGATGCTCTCGACAAAGCCGTTCT-3′	Sadaie *et al.* (2003)
	B15E1-3010	5′-CCATCTCAAACTTCTGTTCAACATT-3′	
mating[a]	mat107FW	5′-TAATATGCTGGTATGGACATAGC-3′	This study
	mat648RV	5′-AGTGGAGATGCGTATTTGGGAAC-3′	

[a] Between the *IR-L* and the *mat 2P*.

sum of a radioactivity of [γ-^{32}P]GTP and $^{32}P_i$ measured by BAS-2500 to 100%, the amount of GTP molecule hydrolyzed per second by Ran was calculated.

Surface Plasmon Resonance Analysis

Measuring was done in a Biacore 2000 (BIAcore, Uppsala, Sweden) instrument. Purified Clr4, and calf H3, were immobilized separately onto the biosensor chip CM5 (BIAcore) with an amine coupling kit (BIAcore). *Sp*Rna1 suspended in HBS-EP buffer (BIAcore) was injected for 180 s. The response of each flow cell from which the response of a blank flow cell was subtracted is indicated. The sensorgrams obtained were evaluated by BIAevaluation software (BIAcore) to estimate the value of k_a and k_d.

Nucleosome Purification

The procedure described by Edmondson *et al.* (1996) was modified as following. Cells in 1 liter of YE5S culture (1×10^7 cells/ml) were grown at 30°C and harvested. Cell pellets were washed with sterile water and then suspended in 50 ml of buffer (0.1 mM Tris, pH 8.5, and 10 mM DTT). After incubation for 10 min at 30°C with gentle shaking, cells were washed with PEMS buffer (100 mM PIPES, pH 6.9, 1 mM EDTA, 1 mM $MgCl_2$, and 1.2 M sorbitol) and suspended in PEMS buffer supplemented with 1.0 mg/ml zymolyase 100T (Seikagaku, Tokyo, Japan). After incubation at 30°C for 30 min with gentle shaking, the reaction was stopped by addition of ice-cold PEMS buffer. Resulting spheroplasts were washed three times with ice-cold PEMS buffer. Cell pellets were suspended in 50 ml of ice-cold NIB buffer (0.25 M sucrose, 60 mM KCl, 14 mM NaCl, 5 mM $MgCl_2$, 1 mM $CaCl_2$, 15 mM PIPES, pH 6.9, and 0.8% Triton X-100) supplemented with a mixture of protease inhibitors (phenylmethylsulfonyl fluoride [code. no. 273-27; Nacalai Tesque, Kyoto, Japan], pepstatin A [code no. 4039; Peptide Institute, Osaka, Japan], leupeptin (code no. 4041; Peptide Institute), aprotinin [code no. 016-11836; Wako Pure Chemicals, Osaka, Japan], and benzamidine (code no. 04036-72; Nacalai Tesque]) on ice for 20 min. After incubation, the insoluble fraction was spun down. Resulting precipitates were washed five times with washing buffer A (10 mM Tris, pH 7.5, 0.5% NP-40, 75 mM NaCl, and a mixture of protease inhibitors) and then incubated in washing buffer B (10 mM Tris, pH 7.5, 0.4 M NaCl, and a mixture of protease inhibitors) for 10 min on ice. After centrifugation, pellets were washed five times with washing buffer B. Both precipitated fractions, P1 and P2, shown in Figure 3A, were digested with 6 U/ml micrococcal nuclease (MNase; catalog no. N3755; Sigma-Aldrich) in MNase buffer {20 mM Tris, pH 7.5, 100 mM KCl, 2 mM $CaCl_2$, 2 mM $MgCl_2$, 5% glycerol, and 0.1% Triton X-100) at 30°C for 1 h. After treatment with MNase, samples were centrifuged to fractionate into the supernatants and the precipitates. The antibodies to *Sp*Rna1 were prepared, and other antibodies were obtained as follows: anti-Pim1 and anti-Spi1 antibodies were from Dr. Shelley Sazer (Baylor College of Medicine, Houston, TX) (Matynia *et al.*, 1996), antihistone H3 antibodies were from Abcam (ab1791; Abcam, Cambridge, United Kingdom), and the monoclonal antibody (mAb) to nucleoporins, mAb414, was from Covance {catalog no. MMS-120R; Covance, Berkeley, CA: Davis and Blobel, 1986).

Chromatin Immunoprecipitation (ChIP) Assay

The procedure described by Hecht *et al.* (1996) was modified as follows. Cells in 100 ml of EMM with supplements culture (1×10^7 cells/ml) grown at 26°C were fixed by incubating with formaldehyde (final concentration 1%) for 15 min at 30°C and then on ice for 50 min. Fixed cells were washed four times with Tris-buffered saline (25 mM Tris, pH 7.5, and 150 mM NaCl). Resulting cells were suspended in 500 μl of extraction buffer (50 mM Tris, pH 7.5, 140 mM NaCl, 1 mM EDTA, 1% Triton X-100, 0.1% Na-deoxycholate, and protease inhibitors) and disrupted with glass beads. Chromatin DNA was fragmented to an average length of 0.8 kb by sonication. Seventy microliters of cell extracts was mixed with antibodies to K9-methylated H3 (catalog no. 07-441; Upstate Biotechnology, Lake Placid, NY), *Sp*Rna1, Swi6 (Sadaie *et al.*, 2004), K4-methylated H3 (ab7766; Abcam), Pim1, or as a control, to mouse immunoglobulin (code no. Z0109; DakoCytomation, Glostrup, Denmark). The immune complexes were purified using protein G-Sepharose beads (GE Healthcare), washed five times with extraction buffer and two times with LiCl buffer (10 mM Tris, pH 8.0, 250 mM LiCl, 1 mM EDTA, 0.5% NP-40, and 0.5% Na-deoxycholate), and then with TE buffer (10 mM Tris, pH 8.0, and 1 mM EDTA). Whole cell extracts (WCE) and the chromatin DNA immunoprecipitated with antibodies were treated with ChEB buffer (10 mM Tris, pH 8.0, 300 mM NaCl, 5 mM EDTA, and 0.5% SDS) for 13 h at 65°C and digested with 10 μg/ml RNase A (Nacalai Tesque) for 30 min at 37°C and then with 80 μg/ml proteinase K (Merck, Darmstadt, Germany) for 1 h at 55°C. Resulting supernatants were given 50 μg of yeast tRNA (catalog no. 109495; Roche Diagnostics) and treated with phenol/chloroform. Purified DNA was precipitated by ethanol in the presence of Na-acetate. Immunoprecipitated DNA and the DNA from WCE were amplified by PCR using the indicated primers (Table 3) in the presence of [α-^{32}P]dCTP. PCR products were separated on 5.0% nondenaturing polyacrylamide gel to be analyzed using BAS-2500.

Preparation of hht1$^+$ for Expressing in S. pombe

The *hht1*$^+$ gene was amplified from *S. pombe* genomic DNA by PCR using the primers H3-REPN (5′-CGG GAT CCA TGG CTC GTA CTA AAC AAA C) and H3-REPC (5′-CGC TCG AGT TAT GAG CGT TCG CCA CGG A). Resulting DNA fragments were introduced into pREP3X (Table 2). To construct the *FLAG-NES* fused *hht1*$^+$ gene, two oligonucleotides—FLAG-NES (5′-CTA GAC TCG AGA TGG ACT ATA AAG ATG ACG ATG ACA AGG GGC TTG CGC TAA AAC TCG CCG GCC TCG ATA TCC A) and FLAG-NESr (5′-TAT GGA TAT CGA GGC CGG CGA GTT TTA GCG CAA GCC CCT TGT CAT CGT CAT CTT TAT AGT CCA TCT CGA GT) (Stade *et al.*, 1997)—were annealed and then digested by the restriction enzymes XbaI and NdeI. Resulting DNA fragments were inserted into pET3b-hht1 (Table 2). The XhoI/BamHI DNA fragments of the resulting plasmid were inserted into pREP3X (Table 2), resulting in pREP3X-NES-hht1. Constructed plasmids (Table 2) were introduced into the *clr4*$^+$ and *clr4*Δ strains with electroporation.

RESULTS

SpRna1 Enhances the HMTase Activity of Clr4 through Histone H3

Previously, we found a genetic interaction of *Sp*Rna1 with Clr4-HMTase (Kusano *et al.*, 2004). To confirm this interaction biochemically, recombinant Clr4 and *Sp*Rna1 were prepared and incubated with H3, a specific substrate of the Clr4-HMTase (Rea *et al.*, 2000; Nakayama *et al.*, 2001). Methylated H3 was detected by the radioactivity of H3 labeled with [^{14}C]SAM. Recombinant Clr4 proteins methylated H3 (Figure 1A, lane 3), as reported previously (Nakayama *et al.*, 2001). The level of ^{14}C-labeled H3 was apparently increased by the addition of *Sp*Rna1 (Figure 1A, compare lane 4 with lane 3), whereas *Sp*Rna1 itself had no activity to methylate H3 (Figure 1A, lane 2). To confirm this finding, increasing doses of *Sp*Rna1, and the controls, RanGEF-RCC1, Ran-GTP, or Ran-GDP, were mixed with H3 and Clr4 in the presence

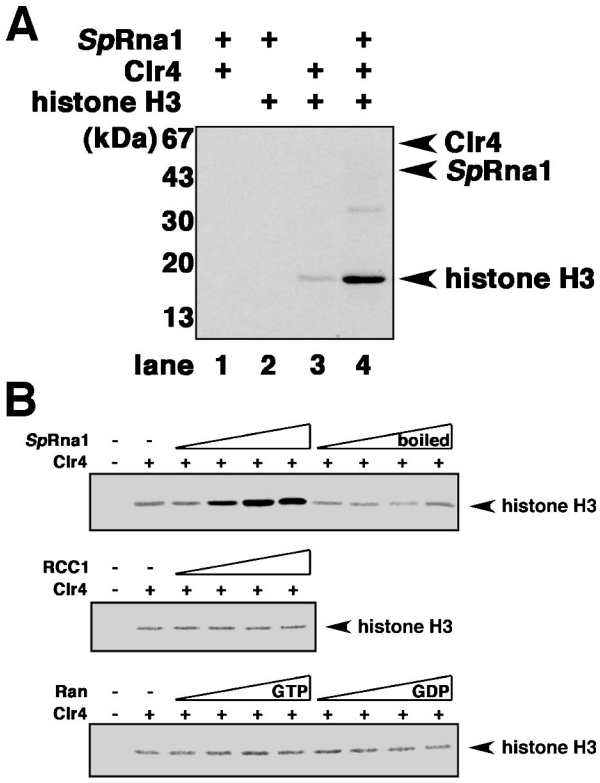

Figure 1. Enhancement of Clr4-HMTase with *Sp*Rna1. (A) Clr4 (80 nM), *Sp*Rna1 (2 μM), and H3 (8 μM) were mixed as indicated and incubated in the presence of [^{14}C]SAM (80 μM) as a methyl donor in 30 μl of HMTase buffer. After incubation for 1 h at 30°C, reaction mixtures were given SDS sample buffer, boiled, and separated by 17% SDS-PAGE and visualized by Coomassie staining. The methylated protein was analyzed using BAS-2500. (B) Clr4 (80 nM) was mixed with H3 (8 μM), [^{14}C]SAM (80 μM), and the increasing amount (20 nM, 200 nM, 2 μM, and 20 μM) of RCC1, Ran that had bound GTP or GDP as indicated, and *Sp*Rna1 in 30 μl of HMTase buffer. Boiled *Sp*Rna1 was also added as a control. After incubation for 1 h at 30°C, reaction mixtures were given SDS sample buffer, boiled, and separated by 17% SDS-PAGE and visualized by Coomassie staining. The methylated H3 was analyzed using BAS-2500.

of [^{14}C]SAM. As shown in Figure 1B, the amount of labeled H3 increased in a dose-dependent manner with the addition of *Sp*Rna1. In contrast, RanGEF-RCC1, Ran-GTP, and Ran-GDP, in addition to the boiled *Sp*Rna1, showed no effect on Clr4-mediated H3 methylation.

The interactions of *Sp*Rna1 with Clr4 and H3 were then examined using surface plasmon resonance analysis. Clr4 and H3 were immobilized separately onto a biosensor chip. When *Sp*Rna1 was injected at the indicated concentration, *Sp*Rna1 bound H3, but not Clr4, in a dose-dependent manner (Figure 2A). The calculated k_a and k_d values of *Sp*Rna1 to H3 were 9.8×10^4 and 4.4×10^{-4}, respectively (equilibrium constant $K_D = 4.5$ nM). H3 consists of the C-terminal core and the N-terminal tail that contains lysine 9 (K9), which is methylated by Clr4 (Nakayama *et al*., 2001; Khan and Hampsey, 2002). To determine which part of H3 binds *Sp*Rna1, an *S. pombe hht1*$^+$ gene encoding a mammalian H3 homologue was cloned and divided into tail and core regions (Figure 2B, top). The full-sized (Hht1-FL), tail (Hht1-tail), and core (Hht1-core) Hht1 produced in *E. coli* were purified and conjugated with Sepharose beads. When these were mixed with *Sp*Rna1, *Sp*Rna1 coprecipitated with the core of Hht1 and with the full-sized Hht1, but not with the tail (Figure 2B). The amount of *Sp*Rna1 coprecipitated with the full-sized Hht1 was similar to the amount coprecipitated with the core (Figure 2B, compare lanes 4 and 6), indicating that *Sp*Rna1 binds to H3 through its core region.

As reported previously (Nakayama *et al*., 2001), Clr4 specifically methylated the H3/Hht1-tail (Figure 2C, open symbols). Under the same conditions, *Sp*Rna1 enhanced the methylation of the full-sized H3, but not the H3/Hht1-tail (Figure 2C). Therefore, we conclude that *Sp*Rna1 enhances Clr4-mediated H3 methylation by binding to the H3-core.

SpRna1 Is Localized on Chromatin

Besides *Sp*Rna1 binding to H3, *Sp*Rna1 enhanced Clr4-HMTase that is required for heterochromatin assembly via H3-K9 methylation. This raises the question of whether *Sp*Rna1 is localized in the nucleus. To address this issue, spheroplasts of exponentially growing wild-type cells were lysed with Triton X-100 to fractionate them into soluble and insoluble fractions (Figure 3A). The insoluble fractions containing chromatin were treated with NP-40 and then with 0.4 M NaCl (Figure 3A). Finally, both precipitated fractions, P1 and P2 (Figure 3A), were digested with MNase. The resulting supernatants and precipitates were analyzed by immunoblotting using the indicated antibodies. Although most *Sp*Rna1 was dissolved after treatment with Triton X-100 as described previously (Feng *et al*., 1999; Dasso, 2002), some *Sp*Rna1 molecules were fractionated into the insoluble fraction containing chromatin (Figure 3B, lane 3). They were rendered soluble after digestion with MNase (Figure 3B, lanes 6 and 10), like Hht1, the *S. pombe* homologue of mammalian H3 used as a control for chromatin-bound protein (Figure 3B, compare *Sp*Rna1 with Hht1). In contrast, Pim1, another chromosomal protein, dissolved after treatment with 0.4 M NaCl, as reported previously for RCC1 (Ohtsubo *et al*., 1989). To confirm our fraction assay, we examined the behavior of nucleoporins by immunoblotting with mAb414, which stains *S. pombe* nucleoporins (Tange *et al*., 2002). Although p65 (designated as *3 in Figure 3B) was soluble, some nucleoporins were insoluble (Figure 3B, mAb414). Among these, proteins designated as *2 dissolved in 400 mM NaCl (Figure 3B, lane 8). In contrast, the nucleoporin designated as *1 partially fractionated into the P2 fraction (Figure 3B, lane 9). However, this was not dissolved by MNase digestion (Figure 3B, compare lane 10 with 11), in contrast to *Sp*Rna1 and Hht1. These results suggest that a nuclear *Sp*Rna1 binds chromatin in a manner similar to H3.

To determine where *Sp*Rna1 associates with chromatin, ChIP assay was carried out on *S. pombe Sprna1*$^+$ and *Sprna1*^{ts} cells, both of which contain the *ura4*$^+$ gene inserted at the innermost repeat of the centromere (*imr1R::ura4*$^+$), and the *ura4 minigene* (*ura4DS/E*). DNA was immunoprecipitated with antibodies to *Sp*Rna1. As controls, we used antibodies to the methylated H3-K9 peptide Swi6 (*S. pombe* homologue of human HP1) and the methylated H3-K4 peptide or Pim1. DNA immunoprecipitated with the antibodies, and DNA of WCE as a control, were subjected to PCR amplification using the primer sets shown in Table 3. These amplified the centromere (*ura4*$^+$ and *dg*223), telomere (*E12*) or mating-type regions. In addition, a primer pair to amplify the *act1*$^+$ gene was included as an internal control to verify the enrichment. A set of *ura4* primers amplified *ura4DS/E*, which can also be used as an internal control, in addition to the *ura4*$^+$ genes inserted in the centromere. The relative enrichment of heterochromatic regions was calculated based on the radioactivity incorporated into PCR products (Noma *et al*., 2001). Autoradiographs of PCR products are shown in Figure 4,

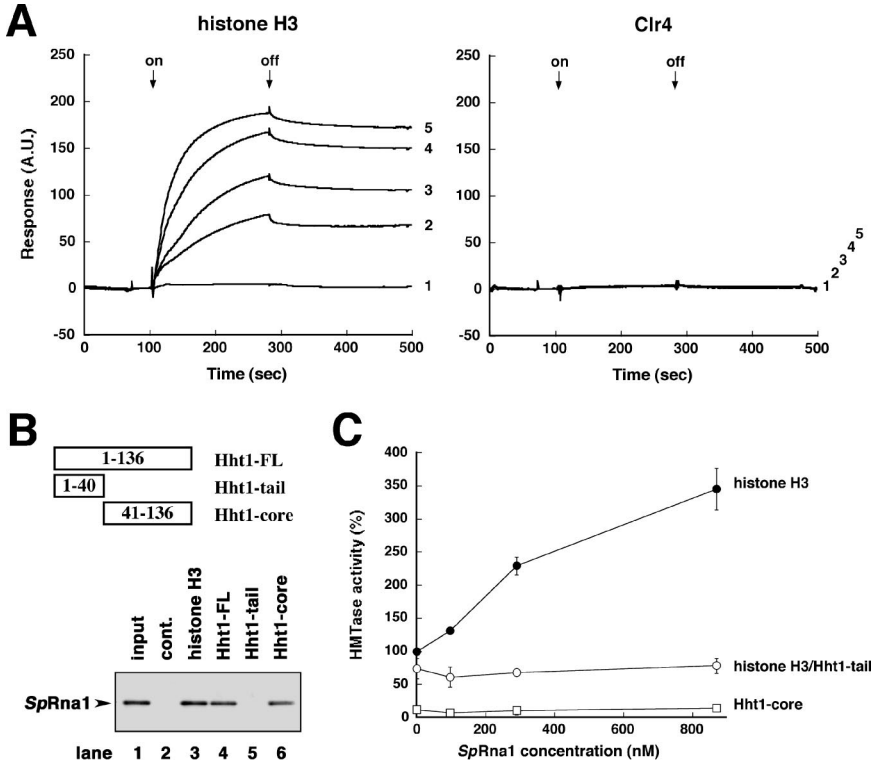

Figure 2. *Sp*Rna1 enhanced the Clr4-HMTase activity through H3. (A) Clr4 and H3 were immobilized separately onto the biosensor chip CM5. The various concentrations of *Sp*Rna1 (1:0, 2:20, 3:60, 4:100, and 5:150 nM) were injected for 180 s (from on to off) in HBS-EP buffer. The responses of flow cells conjugated with H3 and Clr4, from which the response of a blank flow cell had been subtracted, are shown on the vertical line. (B) Top, schematic of *S. pombe* H3, Hht1. Indicated proteins conjugated to Sepharose 4FF beads were incubated with 2 nM 6xHis-*Sp*Rna1 in 1 ml of GAP buffer supplemented with 1 mM CHAPS. After incubation for 1 h at 4°C, beads were spun down, washed five times, and proteins coprecipitated with beads were separated by 5–20% gradient SDS-PAGE and blotted with the mAb to 6xHis (catalog no. 8916-1, Clontech, Mountain View, CA). An arrowhead indicates the position of 6xHis-*Sp*Rna1. Input indicated a total amount of 6xHis-*Sp*Rna1 used in this experiment. (C) Clr4 (80 nM) was mixed in 30 μl of HMTase buffer, with [^{14}C]SAM (80 μM), 8 μM full-sized H3 (●), H3/Hht1-tail* (○), or Hht1-core (□), and an increasing concentration (100, 300, or 900 nM) of *Sp*Rna1 (horizontal line). After incubation for 1 h at 30°C, the reaction mixtures were spotted onto the P81 phosphocellulose filter papers that were washed four times in 50 mM $NaHCO_3$, pH 9.0. The radioactivity incorporated into each substrate was calculated by liquid scintillation counter. The percentage of radioactivity of each substrate labeled with ^{14}C is calculated by setting the radioactivity of the reaction possessing H3, but lacking *Sp*Rna1, to 100% and plotted on the vertical line. The same experiment was repeated three times and error bars were marked. Asterisk (*) indicates that mammalian H3-tail and Hht1-tail possess the same amino acid sequences.

A–D. Unfortunately, we could not detect any PCR products in *Sp*Rna1-ChIP.

SpRna1 Is Required for H3-K9 Methylation in All Heterochromatic Regions of S. pombe

Figure 4 also shows the effect of *Sprna1*^{ts} mutation on H3-K9 methylation and the association of Swi6 with heterochromatin. Even at 26°C, a permissive temperature for *Sprna1*^{ts}, the level of H3-K9 methylation was reduced in all three heterochromatic regions (centromeres, telomere, and the mating-type locus) of *Sprna1*^{ts} compared with *Sprna1*$^{+}$. In particular, H3-K9 methylation was very low at the *imr1R::ura4*$^{+}$ region of *Sprna1*^{ts} (Figure 4A). After incubation at 34°C, a nonpermissive temperature, H3-K9 methylation was further reduced in all three heterochromatic regions of *Sprna1*^{ts} (Figure 4, A–D). In contrast, the levels of H3-K4 methylation at both the *act1*$^{+}$ gene and the *ura4DS/E* minigene were not affected by incubation at 34°C. Thus, a defect of *Sp*Rna1 inhibited H3-K9 methylation in all three heterochromatic regions. In parallel with the reduction of H3-K9 methylation, the level of Swi6 binding the methylated H3-K9 (Bannister *et* al., 2001; Nakayama *et al.*, 2001) was reduced at all three heterochromatic regions of *Sprna1*^{ts} (Figure 4, A–D, Swi6).

It is notable that the level of Swi6 associated with heterochromatin was lower than that of H3-K9 methylation even at 26°C, the permissive temperature (Figure 4, A–D, relative enrichment). Consistent with the fact that the association of Swi6 with methylated H3-K9 is essential for the establishment of heterochromatin, the silencing of the *ura4*$^{+}$ gene inserted into the centromeric region as shown in Figure 4E, top, was abolished in *Sprna1*^{ts}, even at 26°C (Figure 4E).

SpRna1 Enhances the HMTase Activity of Clr4 Independently of Its RanGAP Activity

Because *Sp*Rna1 seems to be involved in heterochromatin assembly, we tested whether the ability of *Sp*Rna1 to enhance the Clr4-mediated H3 methylation could be further increased by the RanGAP activity of *Sp*Rna1. Given that RCC1 showed no effect on the Clr4-mediated H3 methylation (Figure 1B), we constructed a system where Ran-GTP is continuously supplied via RanGEF-RCC1 in the presence of high amounts of GTP, because Ran-GTP is hydrolyzed rapidly to Ran-GDP by the RanGTPase in the presence of *Sp*Rna1–RanGAP (for details, see *Materials and Methods* and legend to Figure 5A legend). In this assay condition, upon adding nonradioactive GTP, the amount of residual [γ-^{32}P]GTP increased (Figure 5A, a), indicating that the exchange Ran-GTP ↔ Ran-GDP occurred continuously in the reaction mixture in which Ran-GTP was mixed with *Sp*Rna1, RCC1, RanBP1, [γ-^{32}P]GTP, and the increasing doses of nonradioactive GTP. The rates of hydrolysis of GTP in the presence of 50 nM RCC1 (open squares) or 500 nM RCC1 (closed circles), were shown as representative results (Figure 5A, b). The optimal reaction mixture in this experiment contained 1000 nM Ran, 500 nM RCC1, 800 nM RanBP1, and 5 mM GTP. In this system, 3.7 pmol of GTP was hydrolyzed per second on average at 250 nM *Sp*Rna1. Even under this Ran-GTP supplying system, the kinetics of the *Sp*Rna1-mediated enhancement of Clr4-HMTase activity was unchanged (Figure 5B, compare −Ran with +Ran). After incubation with increasing doses of *Sp*Rna1 (Figure 5B, horizontal line), a sufficient amount of Ran-GTP was still present (our unpublished data),

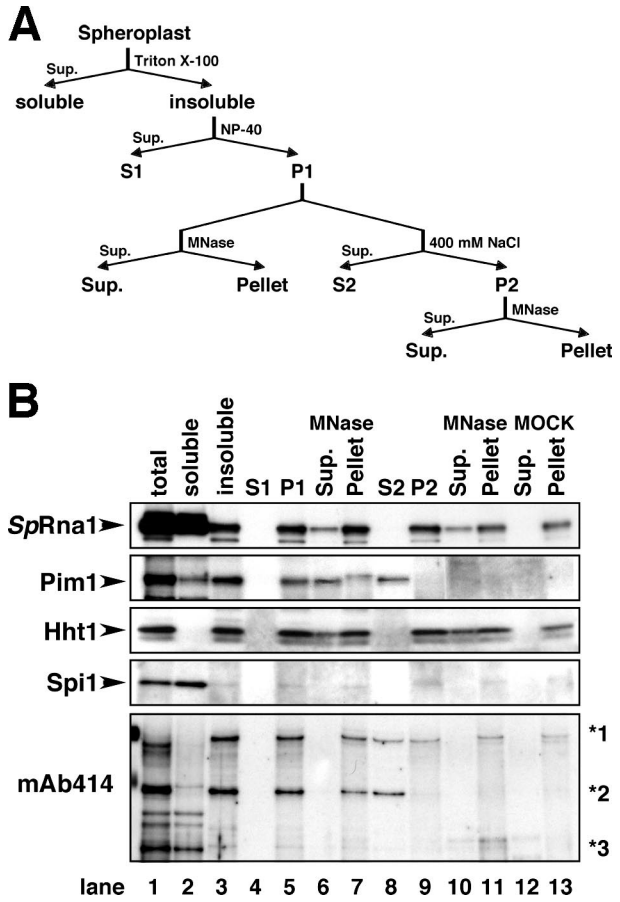

Figure 3. Chromatin-localization of *Sp*Rna1. (A) Schematic of fractionation of the cell extracts derived from spheroplasts of exponentially growing *S. pombe* wild-type AK4. The spheroplasts were treated with Triton X-100. Resulting cell extracts (total) were divided into supernatant (soluble) and precipitate (insoluble) fractions by centrifugation. Resulting insoluble fractions were treated as indicated. At each step, fractions were divided into the supernatants (S) and precipitates (P) by centrifugation. Precipitated fractions that had been treated with MNase were divided into the supernatants (Sup.) and precipitates (Pellet) by centrifugation. (B) Total cell extracts and indicated fractions were resolved in 5–20% gradient SDS-PAGE and analyzed by immunoblotting with antibodies to *Sp*Rna1, Pim1, Hht1, and Spi1 and with mAb414 as indicated. Based on the molecular mass, *1, *2, and *3 may include Nup189 (SPAC1885.12c), Nup124 (SPAC30D11.04c), and p65 (SPAC18B5.08c), respectively.

revealing that *Sp*Rna1 enhances Clr4-mediated H3 methylation independent of RanGAP activity. Indeed, this Clr4-mediated H3 methylation was enhanced by the mutated *Sp*Rna1^{ts} proteins, which did not show any detectable RanGAP activity (Figure 5, B and C).

Histones Inhibit the RanGAP Activity of SpRna1

The nuclear localization of RanGAP led us to test how nuclear RanGAP activity could be inhibited to keep the concentration gradient of Ran-GTP from the nucleus to the cytoplasm. Histone H2, binding RCC1, enhances the RanGEF activity of RCC1 (Nemergut *et al.*, 2001). Based on this report, we studied the effects of core histones on *Sp*Rna1–RanGAP activity. First, we examined whether the core histones, including H3, bound *Sp*Rna1. The indicated histones and bovine serum albumin (BSA) as a control were conjugated with Sepharose beads and then incubated with His-tagged *Sp*Rna1. When the beads were spun down, *Sp*Rna1 coprecipitated significantly with all of the histones, compared with BSA and with beads alone (Figure 6A). Among the histones, H3 and H2B efficiently coprecipitated with *Sp*Rna1. Based on these results, H2B and H4, in addition to H3, were chosen to investigate the effects of histones on the RanGAP activity of *Sp*Rna1. When an increasing dose of histones was incubated with a fixed amount of *Sp*Rna1 (0.5 nM), H3 most efficiently inhibited the RanGAP activity of *Sp*Rna1 (Figure 6B); this was expected because H3 bound *Sp*Rna1 strongly. However, H4 bound *Sp*Rna1 less strongly than H2B but inhibited the RanGAP activity of *Sp*Rna1 more efficiently than H2B. The same results were obtained when an increasing dose of *Sp*Rna1 was incubated with a fixed amount (100 nM) of histones (Figure 6C, open symbols). These results raised the question whether the ability of histones to bind *Sp*Rna1 is important for inhibiting the RanGAP activity of *Sp*Rna1. To study this, *S. pombe* H3, Hht1 (Hht1-FL), and its core (Hht1-core) or tail (Hht1-tail) was incubated with *Sp*Rna1. The Hht1-core, which binds *Sp*Rna1, inhibited the RanGAP activity like the full-sized Hht1 (Figure 6D, −Clr4), but the Hht1-tail, which does not bind *Sp*Rna1, could not. Thus, the binding ability of histones to *Sp*Rna1 was important to inhibit *Sp*Rna1–RanGAP activity, but it may not be sufficient, because H2B did not inhibit the *Sp*Rna1–RanGAP activity significantly. This might explain why a large molar excess of H3 was required to inhibit *Sp*Rna1–RanGAP activity, which was unexpected from the K_D of *Sp*Rna1 to H3 calculated from surface plasmon resonance analysis (Figure 2A). In general, the value of K_D means the binding affinity itself, but it does not always indicate the enzymatic K_m or K_i values.

Because many positively charged amino acid residues were retained in the H3/Hht1-tail, compared with the Hht1-core, positive charge per se might not cause histones to bind and inhibit *Sp*Rna1; the mechanism is presently unknown. Regardless, we conclude that the RanGAP activity of a nuclear *Sp*Rna1 is inhibited by core histones.

Clr4 Abolishes H3-mediated RanGAP Inhibition

The effect of Clr4 on histone-mediated RanGAP inhibition was examined, because overexpression of Clr4 suppresses *Sprna1*^{ts} (Kusano *et al.*, 2004). When Clr4 was added to the mixture of *Sp*Rna1 and histones, the inhibitory effects of H2B and H4 on the RanGAP activity of *Sp*Rna1 were reduced partially but only that of H3 was abolished (Figure 6, C and D, +Clr4). Consistent with these results, Clr4 was spun down with *Sp*Rna1-conjugated Sepharose beads only in the presence of H3 (Figure 6E). Because Clr4 itself showed no ability to enhance the RanGAP activity of *Sp*Rna1 (Figure 6C, closed circles), we then determined how Clr4 could compromise the H3-mediated RanGAP inhibition. A simple idea is that Clr4 released *Sp*Rna1 from H3 by competing for binding H3. To test this, Sepharose beads conjugated with H3 were mixed with *Sp*Rna1 and increasing doses of Clr4. After incubation on ice for 60 min, beads were spun down. Consistent with the result shown in Figure 6E, both Clr4 and *Sp*Rna1 coprecipitated with H3 (Figure 7A, lane 6). However, the amount of *Sp*Rna1 coprecipitated with H3 was not reduced by the addition of an increasing dose of Clr4 (Figure 7A, lane 7), indicating that Clr4 did not release *Sp*Rna1 from H3. This result suggests that Clr4 makes a trimeric complex by binding to the H3 and *Sp*Rna1, as shown in Figure 7C. To study this, *Sp*Rna1-conjugated Sepharose beads were initially mixed with H3 as indicated in Figure 7B, lanes 2–5, and then the beads were spun down. After washing, the precipitated beads were mixed with Clr4 (Figure 7B, lanes 6–9). When beads were again spun down after incubation,

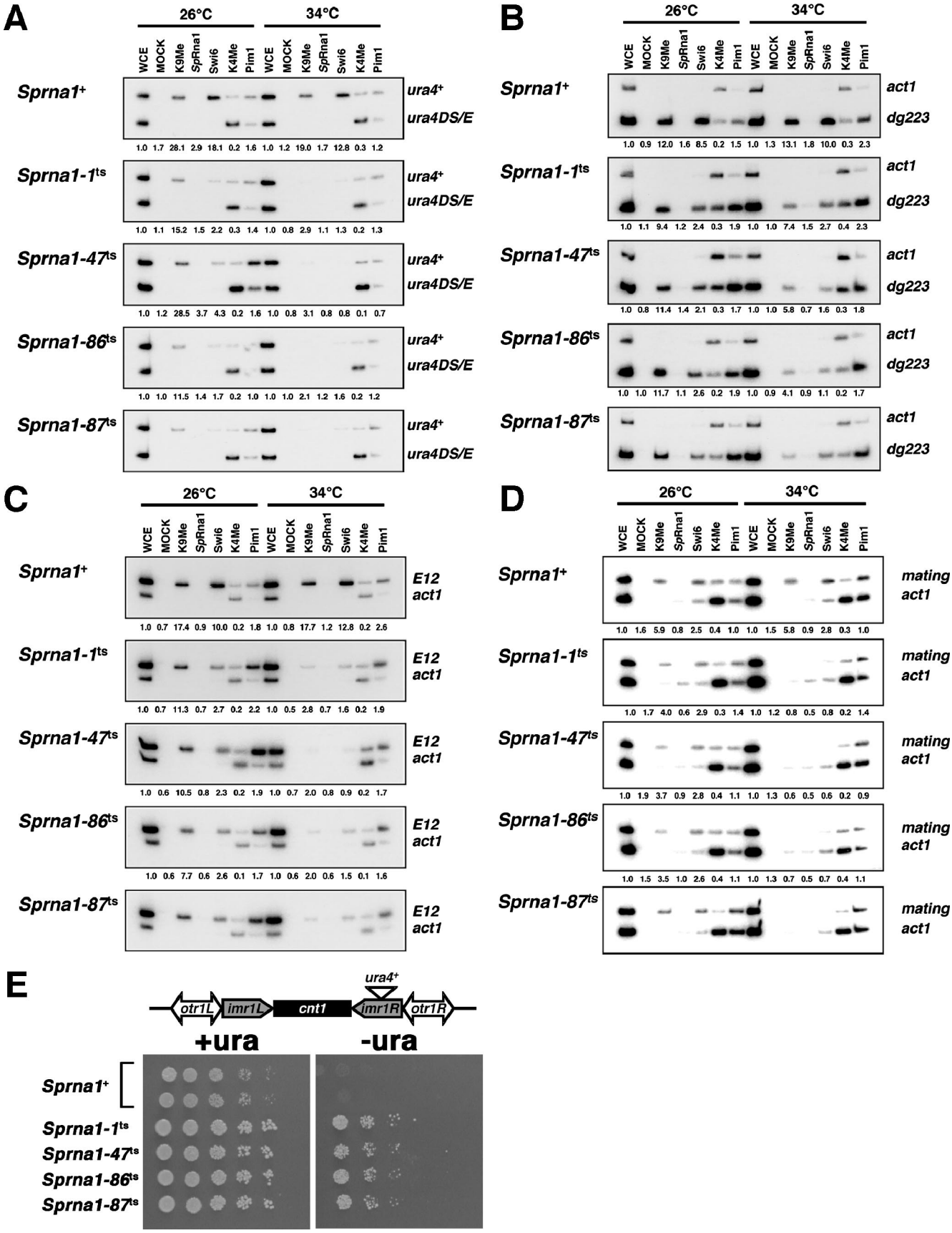
A
26°C
34°C
WCE MOCK K9Me SpRna1 Swi6 K4Me Pim1 WCE MOCK K9Me SpRna1 Swi6 K4Me Pim1
Sprna1+
ura4+
ura4DS/E
1.0 1.7 28.1 2.9 18.1 0.2 1.6 1.0 1.2 19.0 1.7 12.8 0.3 1.2
Sprna1-1ts
ura4+
ura4DS/E
1.0 1.1 15.2 1.5 2.2 0.3 1.4 1.0 0.8 2.9 1.1 1.3 0.2 1.3
Sprna1-47ts
ura4+
ura4DS/E
1.0 1.2 28.5 3.7 4.3 0.2 1.6 1.0 0.8 3.1 0.8 0.8 0.1 0.7
Sprna1-86ts
ura4+
ura4DS/E
1.0 1.0 11.5 1.4 1.7 0.2 1.0 1.0 2.1 1.2 1.6 0.2 1.2
Sprna1-87ts
ura4+
ura4DS/E
B
26°C
34°C
WCE MOCK K9Me SpRna1 Swi6 K4Me Pim1 WCE MOCK K9Me SpRna1 Swi6 K4Me Pim1
Sprna1+
act1
dg223
1.0 0.9 12.0 1.6 8.5 0.2 1.5 1.0 1.3 13.1 1.8 10.0 0.3 2.3
Sprna1-1ts
act1
dg223
1.0 1.1 9.4 1.2 2.4 0.3 1.9 1.0 1.0 7.4 1.5 2.7 0.4 2.3
Sprna1-47ts
act1
dg223
1.0 0.8 11.4 1.4 2.1 0.3 1.7 1.0 1.0 5.8 0.7 1.6 0.3 1.8
Sprna1-86ts
act1
dg223
1.0 1.0 11.7 1.1 2.6 0.2 1.9 1.0 0.9 4.1 0.9 1.1 0.2 1.7
Sprna1-87ts
act1
dg223
C
26°C
34°C
WCE MOCK K9Me SpRna1 Swi6 K4Me Pim1 WCE MOCK K9Me SpRna1 Swi6 K4Me Pim1
Sprna1+
E12
act1
1.0 0.7 17.4 0.9 10.0 0.2 1.8 1.0 0.8 17.7 1.2 12.8 0.2 2.6
Sprna1-1ts
E12
act1
1.0 0.7 11.3 0.7 2.7 0.2 2.2 1.0 0.5 2.8 0.7 1.6 0.2 1.9
Sprna1-47ts
E12
act1
1.0 0.6 10.5 0.8 2.3 0.2 1.9 1.0 0.7 2.0 0.8 0.9 0.2 1.7
Sprna1-86ts
E12
act1
1.0 0.6 7.7 0.6 2.6 0.1 1.7 1.0 0.6 2.0 0.6 1.5 0.1 1.6
Sprna1-87ts
E12
act1
D
26°C
34°C
WCE MOCK K9Me SpRna1 Swi6 K4Me Pim1 WCE MOCK K9Me SpRna1 Swi6 K4Me Pim1
Sprna1+
mating
act1
1.0 1.6 5.9 0.8 2.5 0.4 1.0 1.0 1.5 5.8 0.9 2.8 0.3 1.0
Sprna1-1ts
mating
act1
1.0 1.7 4.0 0.6 2.9 0.3 1.4 1.0 1.2 0.8 0.5 0.8 0.2 1.4
Sprna1-47ts
mating
act1
1.0 1.9 3.7 0.9 2.8 0.4 1.1 1.0 1.3 0.6 0.5 0.6 0.2 0.9
Sprna1-86ts
mating
act1
1.0 1.5 3.5 1.0 2.6 0.4 1.1 1.0 1.3 0.7 0.5 0.7 0.4 1.1
Sprna1-87ts
mating
act1
E
ura4+
otr1L
imr1L
cnt1
imr1R
otr1R
+ura
-ura
Sprna1+
Sprna1-1ts
Sprna1-47ts
Sprna1-86ts
Sprna1-87ts

Figure 4.

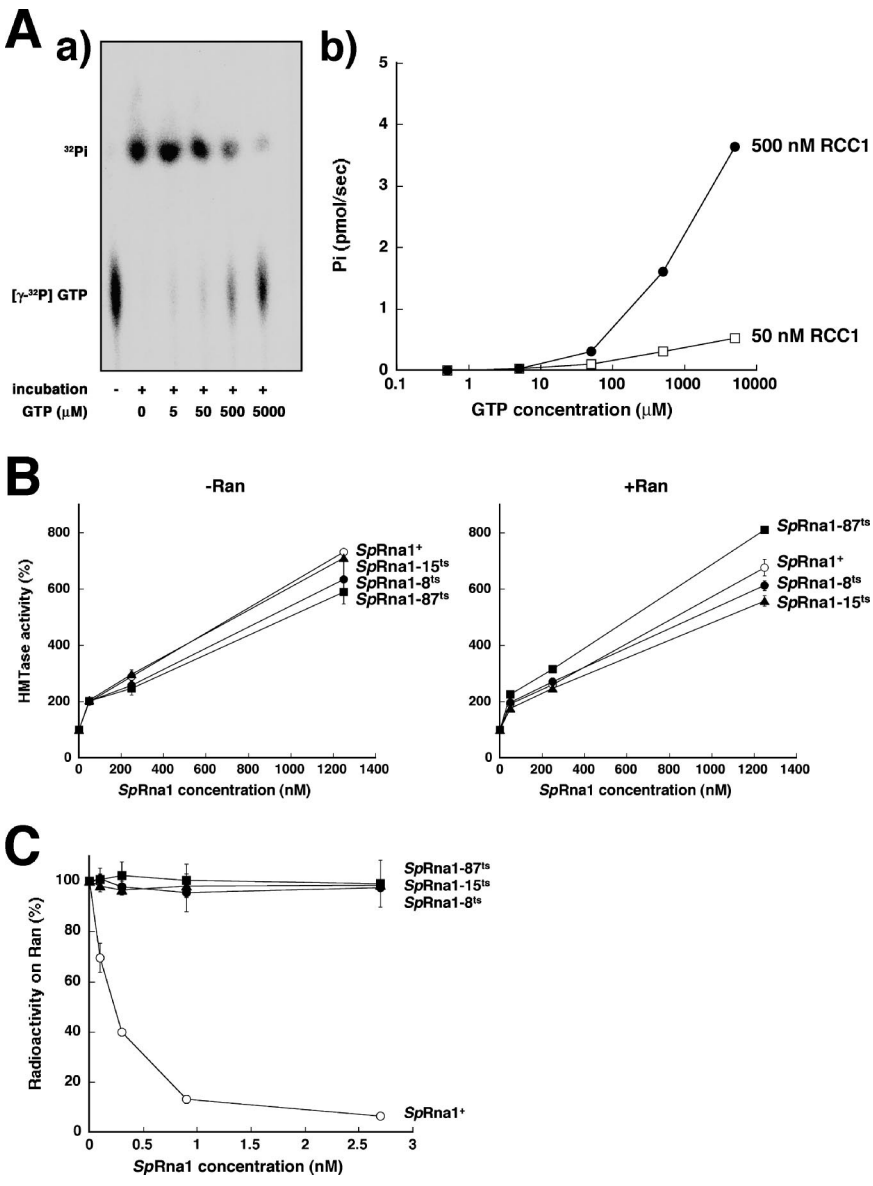

Figure 5. *Sp*Rna1 enhanced H3-K9 methylation independently of its RanGAP activity. (A) Construction of the continuous supplying system of Ran-GTP. (a) 1000 nM Ran-GTP was incubated with *Sp*Rna1 (250 nM), RCC1 (500 nM), RanBP1 (800 nM), and [γ-^{32}P]GTP in the presence of the various concentrations of GTP (0, 5, 50, 500, or 5000 μM) in 30 μl of HMTase buffer for 1 h at 30°C. After incubation, the reaction was stopped by the addition of EDTA (final concentration 72 mM) and boiled. Resulting [γ-^{32}P]GTP and $^{32}P_i$ were separated by thin layer chromatography with 1 M LiCl and 1 M formic acid. ^{32}P-labeled reagents were detected and analyzed using BAS-2500. (b) GTP hydrolysis carried out in the mixture containing of 1000 nM Ran, 800 nM RanBP1, an indicated concentration of GTP, 250 nM *Sp*Rna1, and 50 nM (□) or 500 nM RCC1 (●). $^{32}P_i$ derived by hydrolysis of [γ-^{32}P]GTP that were detected and analyzed using BAS-2500 are shown on the vertical line. Radioactivity of [γ-^{32}P]GTP and $^{32}P_i$ was measured using BAS-2500 for setting the sum of the radioactivity of [γ-^{32}P]GTP and $^{32}P_i$ to 100%. By estimating what percentage of [γ-^{32}P]GTP is hydrolyzed in each reaction mixture, how many molecules of GTP were hydrolyzed in the reaction was calculated. (B) Enhancement of Clr4-HMTase with *Sp*Rna1 in the absence or presence of Ran-GTP. Clr4 (80 nM) was mixed in 30 μl of HMTase buffer with H3 (8 μM) and [^{14}C]SAM (80 μM) in the presence of increasing amount (0, 50, 250, or 1250 nM) of *Sp*Rna1^{+} (○), *Sp*Rna1-8^{ts} (●), *Sp*Rna1-15^{ts} (▲), or *Sp*Rna1-87^{ts} (■) under the continuous supply of Ran-GTP (+Ran) or not (−Ran). After incubation for 1 h at 30°C, the reaction mixtures were boiled in SDS sample buffer and resolved by 17% SDS-PAGE. The bands of H3 were visualized by Coomassie staining. Methylated H3 was analyzed using BAS-2500. The percentage of enzyme activity is plotted, setting the radioactivity in the reaction lacking *Sp*Rna1 to 100% (vertical line). (C) RanGAP activity of *Sp*Rna1^{ts}. Fifty nanomolar Ran-[γ-^{32}P]GTP was incubated in 100 μl of GAP buffer with various concentrations (0, 0.1, 0.3, 0.9, and 2.7 nM) of *Sp*Rna1^{+} (○), *Sp*Rna1-8^{ts} (●), *Sp*Rna1-15^{ts} (▲), or *Sp*Rna1-87^{ts} (■). The reaction mixture was stopped by addition of ice-cold stop buffer. Resulting reaction mixtures were spotted onto the nitrocellulose membrane and washed with stop buffer. The radioactivity of the [γ-^{32}P]GTP remaining on Ran was calculated by a liquid scintillation counter, which was shown as a ratio (percentage) by setting the radioactivity of a sample that was not incubated to 100% on the vertical line. The same experiments were repeated three times and error bars were marked in B and C.

Figure 4 (facing page). *Sp*Rna1 was required for hetrochromain assembly. (A–D) H3-K9 methylation at *CEN*, *TEL*, and *MAT* was reduced in *Sprna1*^{ts}. DNA isolated from the immunoprecipitated chromatin fractions using the indicated antibodies or from the WCE was used as a template for PCR-amplifying *ura4* gene (A), centromeric region (B), telomeric region (C), or mating-type locus (D). The DNA samples were prepared from *Sprna1*$^{+}$ or *Sprna1*^{ts} cells cultured at 26 or 34°C for 5 h. The relative enrichment of *ura4*$^{+}$ to *ura4DS/E* (A) and of *cen-dg223* (B), *tel-E12* (C), or *mating type locus* (D) to *act1* was calculated as reported previously (Noma *et al*., 2001), and its ratio to that of WCE is shown at the bottom of each lane. (E) Centromeric gene silencing activity of *Sprna1*^{ts} mutants. Top, schematic showing the *cen1* and the *ura4*$^{+}$ insertion within *imr1R*. *Sprna1*$^{+}$ and *Sprna1*^{ts} strains possessing the *ura4*$^{+}$ gene at the *imr1R* domain that were spotted. Each strain was grown to 1.0×10^7 cells/ml in EMM supplemented with uracil. Serial dilution (1:5) of the indicated cultures were spotted onto nonselective (+ura) or selective (−ura) plates and incubated at 26°C, the permissive temperature, for 6 d. The highest density spots contained 1×10^4 cells.

the amount of H3 associated with *Sp*Rna1 had not been reduced by the addition of Clr4 (Figure 7B, compare H3 of lane 5 with lane 9). Moreover, Clr4 bound the complex of H3 and *Sp*Rna1 (Figure 7B, lane 9). Thus, a trimeric complex of *Sp*Rna1, H3, and Clr4 (Figure 7C) may form on the chromatin and abolish H3-mediated RanGAP inhibition.

Xpo1/Crm1 Binds SpRna1 in the Presence of H3

Finally, we tested how the nuclear *Sp*Rna1 could be exported to the cytoplasm. Feng *et al*. (1999) suggested that *S. cerevisiae Sc*Rna1p could be exported to the cytoplasm depending on Xpo1p/Crm1p (Weis, 2003), which binds Ran-GTP and various intracellular cargoes, in this case, *Sc*Rna1p. To form an export complex containing Xpo1/Crm1 plus Ran-GTP for *Sc*Rna1p, there must be at least one mediator

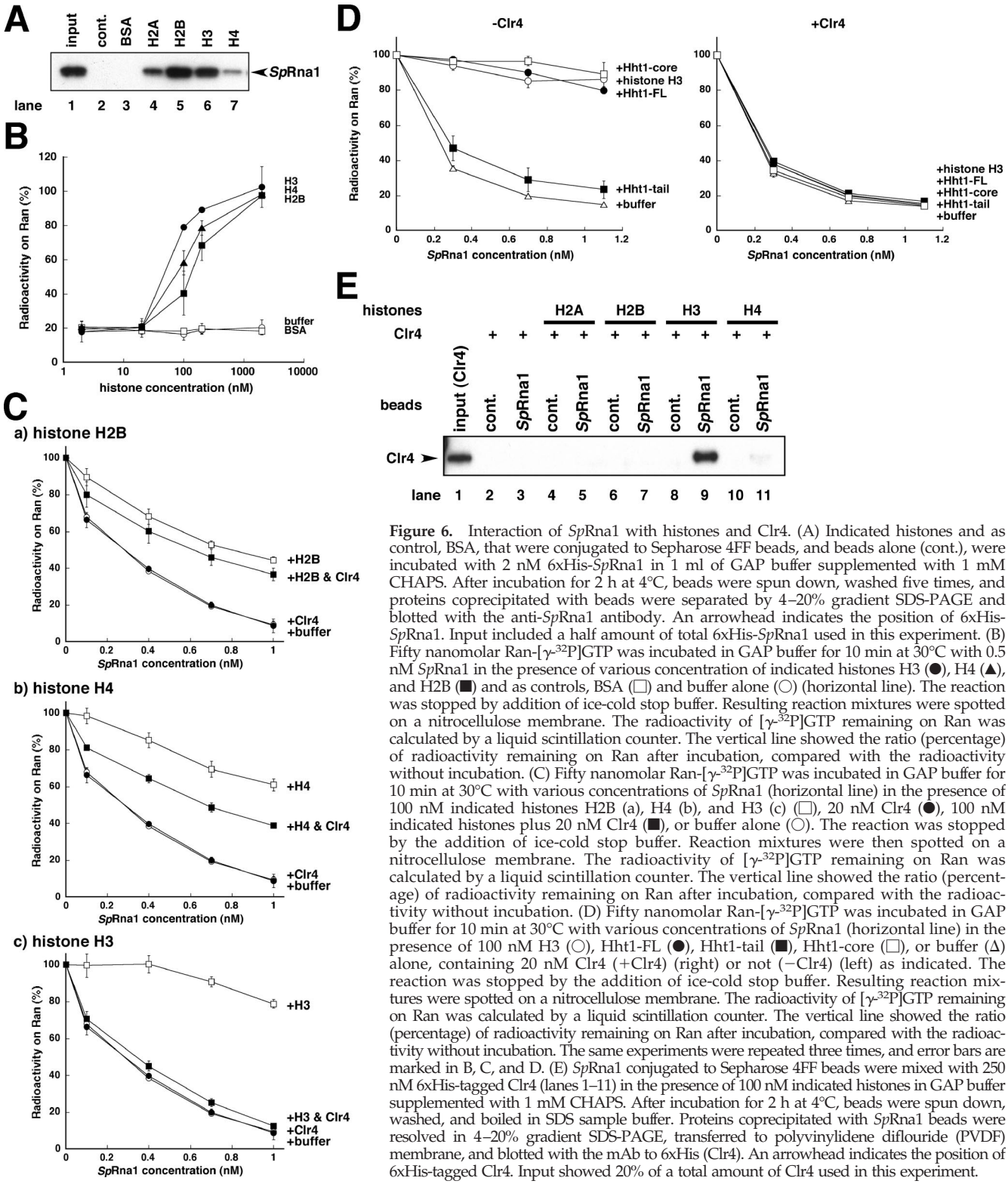

Figure 6. Interaction of *Sp*Rna1 with histones and Clr4. (A) Indicated histones and as control, BSA, that were conjugated to Sepharose 4FF beads, and beads alone (cont.), were incubated with 2 nM 6xHis-*Sp*Rna1 in 1 ml of GAP buffer supplemented with 1 mM CHAPS. After incubation for 2 h at 4°C, beads were spun down, washed five times, and proteins coprecipitated with beads were separated by 4–20% gradient SDS-PAGE and blotted with the anti-*Sp*Rna1 antibody. An arrowhead indicates the position of 6xHis-*Sp*Rna1. Input included a half amount of total 6xHis-*Sp*Rna1 used in this experiment. (B) Fifty nanomolar Ran-[γ-^{32}P]GTP was incubated in GAP buffer for 10 min at 30°C with 0.5 nM *Sp*Rna1 in the presence of various concentration of indicated histones H3 (●), H4 (▲), and H2B (■) and as controls, BSA (□) and buffer alone (○) (horizontal line). The reaction was stopped by addition of ice-cold stop buffer. Resulting reaction mixtures were spotted on a nitrocellulose membrane. The radioactivity of [γ-^{32}P]GTP remaining on Ran was calculated by a liquid scintillation counter. The vertical line showed the ratio (percentage) of radioactivity remaining on Ran after incubation, compared with the radioactivity without incubation. (C) Fifty nanomolar Ran-[γ-^{32}P]GTP was incubated in GAP buffer for 10 min at 30°C with various concentrations of *Sp*Rna1 (horizontal line) in the presence of 100 nM indicated histones H2B (a), H4 (b), and H3 (c) (□), 20 nM Clr4 (●), 100 nM indicated histones plus 20 nM Clr4 (■), or buffer alone (○). The reaction was stopped by the addition of ice-cold stop buffer. Reaction mixtures were then spotted on a nitrocellulose membrane. The radioactivity of [γ-^{32}P]GTP remaining on Ran was calculated by a liquid scintillation counter. The vertical line showed the ratio (percentage) of radioactivity remaining on Ran after incubation, compared with the radioactivity without incubation. (D) Fifty nanomolar Ran-[γ-^{32}P]GTP was incubated in GAP buffer for 10 min at 30°C with various concentrations of *Sp*Rna1 (horizontal line) in the presence of 100 nM H3 (○), Hht1-FL (●), Hht1-tail (■), Hht1-core (□), or buffer (Δ) alone, containing 20 nM Clr4 (+Clr4) (right) or not (−Clr4) (left) as indicated. The reaction was stopped by the addition of ice-cold stop buffer. Resulting reaction mixtures were spotted on a nitrocellulose membrane. The radioactivity of [γ-^{32}P]GTP remaining on Ran was calculated by a liquid scintillation counter. The vertical line showed the ratio (percentage) of radioactivity remaining on Ran after incubation, compared with the radioactivity without incubation. The same experiments were repeated three times, and error bars are marked in B, C, and D. (E) *Sp*Rna1 conjugated to Sepharose 4FF beads were mixed with 250 nM 6xHis-tagged Clr4 (lanes 1–11) in the presence of 100 nM indicated histones in GAP buffer supplemented with 1 mM CHAPS. After incubation for 2 h at 4°C, beads were spun down, washed, and boiled in SDS sample buffer. Proteins coprecipitated with *Sp*Rna1 beads were resolved in 4–20% gradient SDS-PAGE, transferred to polyvinylidene diflouride (PVDF) membrane, and blotted with the mAb to 6xHis (Clr4). An arrowhead indicates the position of 6xHis-tagged Clr4. Input showed 20% of a total amount of Clr4 used in this experiment.

that inhibits the RanGAP activity of *Sc*Rna1p. Our results suggest that H3 plays such a role to export *Sc*Rna1p to the cytoplasm. To test this idea, glutathione *S*-transferase (GST)–fused Xpo1/Crm1 was mixed with *Sp*Rna1^{+}, and as a control, with *Sp*Rna1-87^{ts}, in the presence of Ran-GTP and H3 (Figure 8). When GST-Xpo1/Crm1 beads were spun down in the presence of Ran-GTP alone, *Sp*Rna1-87^{ts} (with very little or no RanGAP activity as shown in Figure 5C) coprecipitated, but *Sp*Rna1^{+} did not (Figure 8, lanes 7 and 18). *Sp*Rna1^{+} coprecipitated with Xpo1/Crm1 in the presence of both Ran-GTP and H3 (Figure 8, lane 20). Thus, it seems that *Sp*Rna1 is exported to the cytoplasm with the aid of H3, in addition to

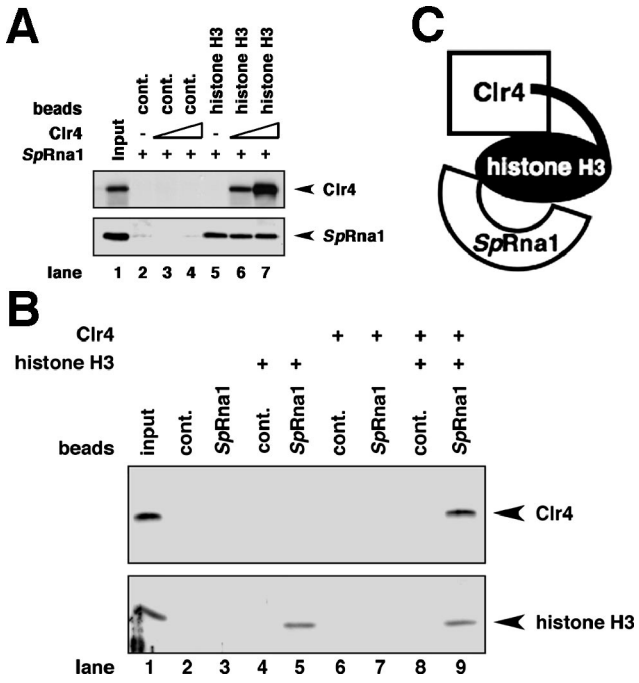

Figure 7. Formation of a complex consisted of *Sp*Rna1, H3, and Clr4. (A) Five hundred pM of 6xHis-tagged *Sp*Rna1 was incubated with mock conjugated Sepharose beads (cont.) and H3-conjugated Sepharose 4FF beads (histone H3) in 100 μl of GAP buffer containing 1 mM CHAPS in the presence of an increasing amount of 6xHis-tagged Clr4 (lanes 3 and 6: 10 nM or lanes 4 and 7: 100 nM). After incubation for 1 h, beads were spun down and boiled in SDS sample buffer. Precipitated proteins were resolved by 5–20% gradient SDS-PAGE and transferred to PVDF membrane. 6xHis-tagged *Sp*Rna1 and Clr4 were detected with the mAb to 6xHis. Input showed a position of *Sp*Rna1 and Clr4 used in this experiment. No proteins were precipitated in the lanes of control (mock-conjugated Sepharose beads). (B) Initially, *Sp*Rna1 conjugated to Sepharose 4FF beads was mixed with or without 250 nM H3 alone in GAP buffer supplemented with 0.2% Tween 20 as indicated (lanes 2–9). After incubation for 1 h at 4°C, beads were spun down, washed, and then mixed with 80 nM 6xHis-tagged Clr4 (lanes 6–9) or not (lanes 2–5) as indicated. After incubation for 1 h at 4°C, beads were spun down, washed, and boiled in SDS sample buffer. Proteins coprecipitated with *Sp*Rna1 beads were resolved in 5–20% gradient (for Clr4) or 17% (for H3) SDS-PAGE and then blotted with the mAb to 6xHis and the anti-H3 antibodies (catalog no. FL-136; Santa Cruz Biotechnology, Santa Cruz, CA). Arrowheads indicate the position of H3 and 6xHis-tagged Clr4, respectively. Input showed a total amount of Clr4 and H3 used in this experiment. (C) Model of interaction of Clr4 with H3 and *Sp*Rna1.

Xpo1/Crm1 plus Ran-GTP. To confirm this, Clr4 was added to a mixture of *Sp*Rna1, Xpo1/Crm1, Ran-GTP and H3. As expected from the finding that Clr4 abolishes the H3-mediated inhibition of RanGAP activity, *Sp*Rna1$^+$ could not interact with Xpo1/Crm1 even in the presence of Ran-GTP and H3, when Clr4 was added (Figure 8, lane 22).

Overexpression of NES-Hht1 Inhibits the Growth of clr4Δ, but Not clr4$^+$, Resulting in Chromosome Missegregation

To test how H3 and Clr4 might regulate *Sp*Rna1 in vivo reciprocally, the *S. pombe* H3 gene *hht1*$^+$ was expressed from the nmt promoter in *S. pombe clr4*Δ and *clr4*$^+$ strains, because our in vitro data suggested that overexpression of H3 could be toxic for the growth of *S. pombe* in the absence of Clr4. The *hht1*$^+$ and *NES-hht1*$^+$ genes, fused with *NES* in-frame,

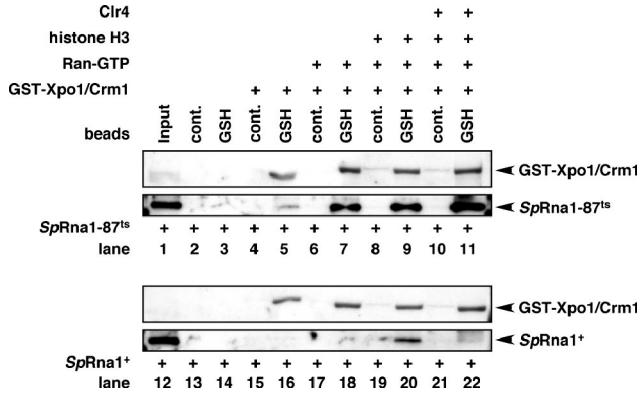

Figure 8. Interaction of *Sp*Rna1 with Xpo1/Crm1. 6xHis (800 pM)-fused *Sp*Rna1$^+$ or *Sp*Rna1-87^{ts} was mixed with Xpo1/Crm1, Ran-GTP, H3, and Clr4 as indicated in GAP buffer supplemented with 1 mM CHAPS. Final concentrations of GST-Xpo1/Crm1, Ran-GTP, H3, and Clr4 used in this assay were 40, 60, 200, and 20 nM, respectively. After 10-min incubation at 30°C, the reaction was stopped by ice-cold GAP buffer containing CHAPS. Glutathione Sepharose 4FF (code no. 17-5132; GE Healthcare) (GSH) or protein G-Sepharose 4FF as a control (cont.) was added to the reaction mixture. After incubation, beads were spun down. Proteins cofractionated with beads were resolved in 5–20% gradient gel and analyzed by blotting with the mAb to 6xHis and the mAb to GST (catalog no. sc-138; Santa Cruz Biotechnology). Input indicated a half amount of *Sp*Rna1$^+$ and *Sp*Rna1-87^{ts} proteins used in this experiment.

were conjugated with the thiamine-regulated *nmt* promoter in the pREP3X plasmid (Table 2) and then introduced into the *clr4*Δ and *clr4*$^+$ strains. Transformants of *clr4*Δ and *clr4*$^+$ containing pREP3X-hht1, pREP3X-NES-hht1, or pREP3X alone were cultivated on synthetic medium plates, with or without thiamine at 30°C. Five days later, the *clr4*Δ cells containing pREP3X-NES-hht1 could not make a clear colony in the absence of thiamine, whereas they papillated in the presence of thiamine. In contrast, *clr4*$^+$ cells containing pREP3X-NES-hht1 papillated even in the absence of thiamine (Figure 9A).

Twenty-four hours after thiamine depletion, the growth of *clr4*Δ cells containing pREP3X-NES-hht1, was retarded (Figure 9B, top left). At that time, NES-Hht1 accumulated in both the nucleus (insoluble) and the cytoplasm (soluble) (Figure 9B, bottom left). The calculated ratio of NES–Hht1 level between the nucleus and the cytoplasm was 2.5:1 (Figure 9B, bottom left), suggesting that both cytoplasmic and nuclear RanGAP could be inhibited. Consistently, cells showing abnormal chromosome segregation, accumulated, similar to *Sprna1*^{ts} (Figure 9B, right, cells indicated by an arrow and an arrowhead). The calculated frequency of *clr4*Δ [pREP3X-NES-hht1] cells showing abnormal chromosomal segregation in total mitotic cells increased compared with *clr4*Δ possessing pREP3X vector alone after 24-h incubation without thiamine (Figure 9C).

DISCUSSION

Here, we found that *S. pombe* RanGAP is localized on the chromatin in addition to cytoplasm, and it seems likely to be involved in heterochromatin assembly.

An Unexpected Function of SpRna1 Enhances Clr4-mediated H3-K9 Methylation Independently of RanGAP Activity

It is very surprising that the recombinant *Sp*Rna1 enhanced HMTase activity of Clr4. Under the same conditions, recombi-

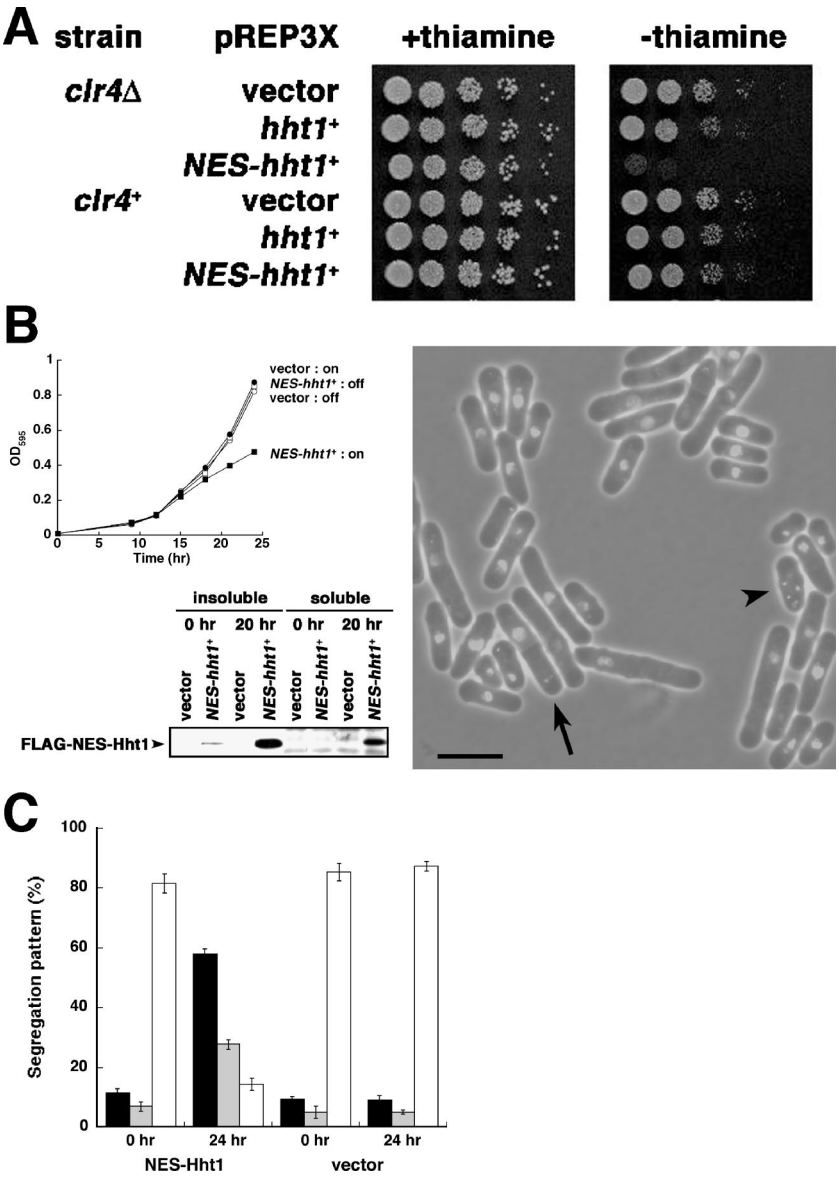

Figure 9. Overexpression of NES-fused *S. pombe hht1*$^+$ was lethal for *clr4*Δ but not for *clr4*$^+$. (A) *clr4*Δ and *clr4*$^+$ cells expressing Hht1, NES-Hht1, or not (vector alone) were grown in EMM supplemented with uracil, adenine, and thiamine to 1.0×10^7 cells/ml. After fivefold serial dilution, cells were spotted onto thiamine additive (+thiamine) or thiamine-free (−thiamine) plates and incubated at 30°C for 5 d. The highest density spots contained 1×10^4 cells. (B) Cultures of *clr4*Δ cells containing pREP3X-NES-hht1 (*NES-hht1*$^+$, rectangle) or pREP3X alone (vector, circle) were diluted to optical density $(O.D.)_{595} = 0.02$ and then incubated in the presence of thiamine (○, □) or not (●, ■). At the indicated time, $O.D._{595}$ values were measured and blotted (top left). After incubation for 24 h, cells were collected, fixed with 3.3% of paraformaldehyde in phosphate-buffered saline, and mounted in VECTASHIELD with 4,6-diamidino-2-phenylindole (Vector Laboratories, Burlingame, CA) to visualize chromosome. Representative cells showing unequal chromosome segregation (arrow) and multinuclei (arrowhead) were indicated in the right photograph. Bar = 10 μm. Bottom left, to verify the expression of FLAG-NES-Hht1, cells (5.0×10^7) containing the indicated plasmid were harvested after incubation for 20 h in the absence of thiamine and then incubated in PEMS buffer supplemented with 1.0 mg/ml zymolyase 100T for 20 min at 30°C. Resulting spheroplasts were treated with 1% NP-40 and then centrifuged. Resulting supernatants and pellets were used as soluble and insoluble chromatin fractions, respectively. Fractions were separated in 17% SDS-PAGE and blotted with the mAb to FLAG M2 (catalog no. F-3165; Sigma-Aldrich). (C) Frequency of mitotic cells. More than 200 mitotic cells were examined three times to calculate the frequency (percentage) of cells showing unequal chromosome segregation (closed bar), multinuclei (hatched bar), and normal mitosis (open bar).

nant Clr4 methylated both full-sized and tail-H3, but not the core of *S. pombe* H3, Hht1, as reported previously (Nakayama *et al.*, 2001). In contrast, *Sp*Rna1 enhanced the methylation of full-sized H3 but not of the H3-tail alone. Thus, *Sp*Rna1 did not directly enhance Clr4-HMTase. From these results combined with *Sp*Rna1 bounding the core of *S. pombe* H3, Hht1, but not the tail of H3/Hht1, we conclude that *Sp*Rna1 enhances the Clr4-mediated H3-K9 methylation via the core region of Hht1. Because *Sp*Rna1 is the *S. pombe* RanGAP, Ran GTPase-activating protein, it was important to determine whether Ran-GTPase is involved in the *Sp*Rna1-mediated Clr4-HMTase enhancement. *Sp*Rna1^{ts}-mutated proteins with no significant RanGAP activity enhanced the Clr4-mediated H3 methylation, similar to *Sp*Rna1$^+$. In addition, we developed an in vitro system in which Ran-GTP was continuously supplied by RanGEF, RCC1, in the presence of a high dose of RanGAP, *Sp*Rna1. However, the ability of *Sp*Rna1 to enhance the Clr4-mediated H3-K9 methylation was unchanged, even in the presence of a sufficient amount of Ran-GTP. Thus, *Sp*Rna1 seems to enhance Clr4-mediated H3-K9 methylation independently of Ran-GTP in vitro.

The critical issue was whether the ability of *Sp*Rna1 to enhance the Clr4-HMTase activity could be observed in vivo. Cell fractionation analysis revealed that *Sp*Rna1 was present in the nucleus as well as the cytoplasm, as suggested by Feng *et al.* (1999). Although nucleoporins were fractionated into the insoluble fraction containing chromatin, they were not dissolved by MNase treatment. In contrast, the nuclear *Sp*Rna1 was dissolved by MNase treatment, similar to H3. Thus, a nuclear *Sp*Rna1 seems to bind chromatin in a manner similar to *S. pombe* H3, Hht1. The level of nuclear *Sp*Rna1 dissolved by MNase treatment seemed to be lower than that of Hht1, suggesting that nuclear *Sp*Rna1 might be localized in chromosomal regions resistant to MNase treatment. In vitro, *Sp*Rna1 bound the core histones, particularly H3 and H2B. Because H3 and H2B form dimers with H4 and H2A, respectively (Luger *et al.*, 1997; Black *et al.*, 2004), it is possible that *Sp*Rna1 is anchored to the chromatin through the core histones. Because *Sp*Rna1 binds to Clr4 in the presence of H3, a nuclear *Sp*Rna1 could make a trimeric complex with H3 and Clr4 to enhance the Clr4-HMTase activity that is essential for heterochromatin assembly. Consistently, *Sprna1*^{ts} showed a defect in heterochro-

matin assembly; compared with H3-K4 methylation, H3-K9 methylation of *Sprna1*^{ts} was strongly reduced after incubation at 34°C at all three heterochromatic regions of *S. pombe*. In parallel with the reduction of H3-K9 methylation, the association of Swi6 with chromatin was inhibited, consistent with the observation that Swi6 binds the methylated H3-K9 (Bannister *et al*., 2001; Nakayama *et al*., 2001). Thus, *Sp*Rna1 seems to be required for H3-K9 methylation in all heterochromatic regions of *S. pombe*. In this context, whether *Sp*Rna1 enhances the Clr4-HMTase activity independently of its RanGAP activity is now questionable, because the *Sprna1*^{ts} mutation should affect the RanGAP activity of *Sp*Rna1. One possibility is that the ability of *Sp*Rna1 to enhance Clr4-HMTase might be affected by the *Sprna1*^{ts} mutation in vivo, in a temperature-dependent manner by an unknown mechanism. In this context, it is notable that the crystal structure of *Sp*Rna1 is highly similar to the ribonuclease inhibitor and to the U2A′ small nuclear ribonucleoprotein (Hillig *et al*., 1999), because several lines of evidence support a role for RNA in the formation of heterochromatin (Maison *et al*., 2002; Grewal and Moazed, 2003). The other puzzle is that the *Sprna1*^{ts} mutation shows a gene-silencing defect at the centromere but not at telomeres (Kusano *et al*., 2004), although all of the heterochromatic regions of *S. pombe* are affected by the *Sprna1*^{ts} mutation. A similar centromere-specific silencing defect has been observed in RNA interference (RNAi) mutant cells (Volpe *et al*., 2002; Hall *et al*., 2003) and *chp1*-deleted cells (Thon and Verhein-Hansen, 2000), whereas both RNAi components and Chp1 are involved in heterochromatin assembly at all three heterochromatic regions of *S. pombe* (Sadaie *et al*., 2004; Kanoh *et al*., 2005; Miller *et al*., 2005). Taz1 (a telomere-associated factor in *Schizosaccharomyces pombe*) is specifically required for the establishment of telomeres but not for that of centromeres in *S. pombe* (Cooper *et al*., 1997; Kanoh *et al*., 2005; Miller *et al*., 2005). The centromere-specific silencing defect observed in *Sprna1*^{ts} cells may reflect such a difference between centromeric and telomeric chromatin.

Histones and Clr4 Reciprocally Regulates Nuclear RanGAP Activity

Our finding that *Sp*Rna1 is localized on the chromatin raised the important general question of how the RanGAP activity of nuclear *Sp*Rna1 is inhibited, otherwise it abolishes the nucleocytoplasmic gradient of Ran-GTP concentration. In this context, it is notable that all core histones bound *Sp*Rna1 and inhibited its RanGAP activity. Among core histones, H3, which cooperates with H4 (Luger *et al*., 1997; Black *et al*., 2004), most strongly inhibited the RanGAP activity of *Sp*Rna1. Thus, we conclude that the RanGAP activity of nuclear *Sp*Rna1 is inhibited by core histones, particularly H3. In contrast, Clr4 abolished the H3-mediated inhibition of *Sp*Rna1–RanGAP activity. This finding raised another question of whether the *Sp*Rna1–RanGAP activity uncovered by Clr4 may play a role in the nucleus, independent of the ability of *Sp*Rna1 to enhance the Clr4-HMTase. It has been reported that Ran can bind to chromatin in manners dependent or independent of RCC1. In the RCC1-independent mode, Ran directly binds both H3 and H4 (Bilbao-Cortes *et al*., 2002). Chromatin-bound Ran, suggested to function for spindle formation and for nuclear envelope assembly, might cooperate with a nuclear RanGAP for Ran-mediated nuclear events. It remains to be determined whether a nuclear RanGAP functions for higher order chromatin assembly through the Ran cycle, as in microtubule assembly and nuclear membrane formation. In this context, it is notable that most *Sprna1*^{ts} mutants do not show detectable defects in nucleocytoplasmic transport or in microtubule assembly. Because the disruption of *clr4*$^{+}$ gene increased the temperature sensitivity of *Sprna1*^{ts}, but it was not lethal for *Sprna1*^{ts} (Kusano *et al*., 2001), a nuclear *Sp*Rna1 might function in an unknown pathway, other than the pathway including Clr4.

The RanGAP activity of a nuclear *Sp*Rna1 should be carefully regulated temporally and spatially to maintain the nucleocytoplasmic gradient of Ran-GTP concentration. After establishment of heterochromatin, a nuclear *Sp*Rna1 would be immediately inactivated or exported to the cytoplasm with the aid of its NES signal. Indeed, *Sp*Rna1 could make a stable complex with Xpo1/Crm1 plus Ran-GTP in the presence of H3. Accordingly, we could not detect any association of *Sp*Rna1 with chromatin by the ChIP assay, whereas a chromatin-bound *Sp*Rna1 was detected by immunoblotting analysis. In conclusion, we suggest that histones, particularly H3, and Clr4 regulate a nuclear *Sp*Rna1 reciprocally for heterochromatin assembly and for its nuclear export.

ACKNOWLEDGMENTS

We thank Drs. Shelley Sazer for the anti-Pim1 and anti-Spi1 antibodies, Kathy Wilson (Johns Hopkins University School of Medicine, Baltimore, MD) for helpful discussion, and Genevieve Almouzni (Institut Curie, Paris, France) for reading this manuscript and for helpful suggestions. This work was supported by grants-in-aid for specially promoted research from the Ministry of Education, Science, Sports and Culture of Japan.

REFERENCES

Bannister, A. J., Zegerman, P., Partridge, J. F., Miska, E. A., Thomas, J. O., Allshire, R. C., and Kouzarides, T. (2001). Selective recognition of methylated lysine 9 on histone H3 by the HP1 chromo domain. Nature *410*, 120–124.

Becker, J., Melchior, F., Gerke, V., Bischoff, F. R., Ponstingl, H., and Wittinghofer, A. (1995). RNA1 encodes a GTPase-activating protein specific for Gsp1p, the Ran/TC4 homologue of *Saccharomyces cerevisiae*. J. Biol. Chem. *270*, 11860–11865.

Bischoff, F. R., Krebber, H., Kempf, T., Hermes, I., and Ponstingl, H. (1995a). Human RanGTPase activating protein RanGAP1 is a homologue of yeast Rna1p involved in mRNA processing and transport. Proc. Natl. Acad. Sci. USA *92*, 1749–1753.

Bischoff, F. R., Krebber, H., Smirnova, E., Dong, W., and Ponstingl, H. (1995b). Co-activation of RanGTPase and inhibition of GTP dissociation by Ran-GTP binding protein RanBP1. EMBO J. *14*, 705–715.

Bischoff, F. R., and Ponstingl, H. (1991). Catalysis of guanine nucleotide exchange on Ran by the mitotic regulator RCC1. Nature *354*, 80–82.

Bilbao-Cortes, D., Hetzer, M., Langst, G., Becker, P. B., and Mattaj, I. W. (2002). Ran binds to chromatin by two distinct mechanisms. Curr. Biol. *12*, 1151–1156.

Black, B. E., Foltz, D. R., Chakravarthy, S., Luger, K., Woods, V. L., and Cleveland, D. W. (2004). Structural determinants for generating centromeric chromatin. Nature *430*, 578–582.

Cooper, J. P., Nimmo, E. R., Allshire, R. C., and Cech, T. R. (1997). Regulation of telomere length and function by a Myb-domain protein in fission yeast. Nature *385*, 744–747.

Dasso, M. (2002). The Ran GTPase: theme and variations. Curr. Biol. *12*, R502–R508.

Dasso, M., Seki, T., Azuma, Y., Ohba, T., and Nishimoto, T. (1994). A mutant form of the Ran/TC4 protein disrupts nuclear function in *Xenopus laevis* egg extracts by inhibiting the RCC1 protein, a regulator of chromosome condensation. EMBO J. *13*, 5732–5744.

Davis, L. I., and Blobel, G. (1986). Identification and characterization of a nuclear pore complex protein. Cell *45*, 699–709.

Edmondson, D. G., Smith, M. M., and Roth, S. Y. (1996). Repression domain of the yeast global repressor Tup1 interacts directly with histones H3 and H4. Genes Dev. *10*, 1247–1259.

Ekwall, K., Olsson, T., Turner, B. M., Cranston, G., and Allshire, R. C. (1997). Transient inhibition of histone deacetylation alters the structural and functional imprint at fission yeast centromeres. Cell *91*, 1021–1032.

Feng, W., Benko, A. L., Lee, J. H., Stanford, D. R., and Hopper, A. K. (1999). Antagonistic effects of NES and NLS motifs determine *S. cerevisiae* Rna1p subcellular distribution. J. Cell Sci. *112*, 339–347.

Grewal, S. I., and Moazed, D. (2003). Heterochromatin and epigenetic control of gene expression. Science *301*, 798–802.

Hall, I. M., Noma, K., and Grewal, S. I. (2003). RNA interference machinery regulates chromosome dynamics during mitosis and meiosis in fission yeast. Proc. Natl. Acad. Sci. USA *100*, 193–198.

Hayashi, N., Yokoyama, N., Seki, T., Azuma, Y., Ohba, T., and Nishimoto, T. (1995). RanBP1, a Ras-like nuclear G protein binding to Ran/TC4, inhibits RCC1 via Ran/TC4. Mol. Gen. Genet. *247*, 661–669.

Hecht, A., Strahl-Bolsinger, S., and Grunstein, M. (1996). Spreading of transcriptional repressor SIR3 from telomeric heterochromatin. Nature *383*, 92–96.

Hetzer, M., Gruss, O. J., and Mattaj, I. W. (2002). The Ran GTPase as a marker of chromosome position in spindle formation and nuclear envelope assembly. Nat. Cell Biol. *4*, E177–E184.

Hillig, R. C., Renault, L., Vetter, I. R., Drell, T., Wittinghofer, A., and Becker, J. (1999). The crystal structure of rna1p: a new fold for a GTPase-activating protein. Mol. Cell *3*, 781–791.

Kai, R., Ohtsubo, M., Sekiguchi, T., and Nishimoto, T. (1986). Molecular cloning of a human gene that regulates chromosome condensation and is essential for cell proliferation. Mol. Cell. Biol. *6*, 2027–2032.

Kalab, P., Weis, K., and Heald, R. (2002). Visualization of a Ran-GTP gradient in interphase and mitotic *Xenopus* egg extracts. Science *295*, 2452–2456.

Kanoh, J., Sadaie, M., Urano, T., and Ishikawa, F. (2005). Telomere binding protein Taz1 establishes Swi6 heterochromatin independently of RNAi at telomeres. Curr. Biol. *16*, 1808–1819.

Khan, A. U., and Hampsey, M. (2002). Connecting the DOTs: covalent histone modifications and the formation of silent chromatin. Trends Genet. *18*, 387–389.

Kusano, A., Staber, C., and Ganetzky, B. (2001). Nuclear mislocalization of enzymatically active RanGAP causes segregation distortion in *Drosophila*. Dev. Cell *1*, 351–361.

Kusano, A., Yoshioka, T., Nishijima, H., Nishitani, H., and Nishimoto, T. (2004). *Schizosaccharomyces pombe* RanGAP homolog, SpRna1, is required for centromeric silencing and chromosome segregation. Mol. Biol. Cell *15*, 4960–4970.

Kunzler, M., Gerstberger, T., Stutz, F., Bischoff, F. R., and Hurt, E. (2000). Yeast Ran-binding protein 1 (Yrb1) shuttles between the nucleus and cytoplasm and is exported from the nucleus via a CRM1 (XPO1)-dependent pathway. Mol. Cell. Biol. *20*, 4295–4308.

Luger, K., Mader, A. W., Richmond, R. K., Sargent, D., and Richmond, T. J. (1997). Crystal structure of the nucleosome core particle at 2.8 A resolution. Nature *389*, 251–260.

Luger, K., Rechsteiner, T. J., and Richmond, T. J. (1999). Preparation of nucleosome core particle from recombinant histones. Methods Enzymol. *304*, 3–19.

Lyttle, T. W. (1991). Segregation distorters. Annu. Rev. Genet. *25*, 511–557.

Maison, C., Bailly, D., Peters, A. H., Quivy, J. P., Roche, D., Taddei, A., Lachner, M., Jenuwein, T., and Almouzni, G. (2002). Higher-order structure in pericentric heterochromatin involves a distinct pattern of histone modification and an RNA component. Nat. Genet. *30*, 329–334.

Matynia, A., Dimitrov, K., Mueller, U., He, X., and Sazer, S. (1996). Perturbations in the spi1p GTPase cycle of *Schizosaccharomyces pombe* through its GTPase-activating protein and guanine nucleotide exchange factor components result in similar phenotypic consequences. Mol. Cell. Biol. *16*, 6352–6362.

Mattaj, I. (2004). Sorting out the nuclear envelope from the endoplasmic reticulum. Nat. Rev. Mol. Cell. Biol. *5*, 65–69.

Maundrell, K. (1993). Thiamine-repressible expression vectors pREP and pRIP for fission yeast. Gene *123*, 127–130.

Merrill, C., Bayraktaroglu, L., Kusano, A., and Ganetzky, B. (1999). Truncated RanGAP encoded by the segregation distorter locus of *Drosophila*. Science *283*, 1742–1745.

Miller, K. M., Ferreira, M. G., and Cooper, J. P. (2005). Taz1, Rap1 and Rif1 act both interdependently and independently to maintain telomeres. EMBO J. *24*, 3128–3135.

Moore, J. D. (2001). The Ran-GTPase and cell-cycle control. Bioessays *23*, 77–85.

Nakagawa, H., Lee, J. K., Hurwitz, J., Allshire, R. C., Nakayama, J., Grewal, S. I., Tanaka, K., and Murakami, Y. (2002). Fission yeast CENP-B homologs nucleate centromeric heterochromatin by promoting heterochromatin-specific histone tail modifications. Genes Dev. *16*, 1766–1778.

Nakayama, J., Rice, J. C., Strahl, B. D., Allis, C. D., and Grewal, S. I. (2001). Role of histone H3 lysine 9 methylation in epigenetic control of heterochromatin assembly. Science *292*, 110–113.

Nemergut, M. E., Mizzen, C. A., Stukenberg, T., Allis, C. D., and Macara, I. G. (2001). Chromatin docking and exchange activity enhancement of RCC1 by histones H2A and H2B. Science *292*, 1540–1543.

Noguchi, E., Hayashi, N., Nakashima, N., and Nishimoto, T. (1997). Yrb2p, a Nup2p-related yeast protein, has a functional overlap with Rna1p, a yeast Ran-GTPase-activating protein. Mol. Cell. Biol. *17*, 2235–2246.

Noma, K., Allis, D. A., and Grewal, S. S. (2001). Transitions in distinct histone H3 methylation patterns at the heterochromatin domain boundaries. Science *293*, 1150–1155.

Ohtsubo, M., Okazaki, H., and Nishimoto, T. (1989). The RCC1 protein, a regulator for the onset of chromosome condensation locates in the nucleus and binds to DNA. J. Cell Biol. *109*, 1389–1397.

Rea, S., *et al*. (2000). Regulation of chromatin structure by site-specific histone H3 methyltransferases. Nature *406*, 593–599.

Sadaie, M., Iida, T., Urano, T., and Nakayama, J. (2004). A chromodomain protein, Chp1, is required for the establishment of heterochromatin in fission yeast. EMBO J. *23*, 3825–3835.

Seino, H., Hisamoto, N., Uzawa, S., Sekiguchi, T., and Nishimoto, T. (1992). DNA-binding domain of RCC1 protein is not essential for coupling mitosis with DNA replication. J. Cell Sci. *102*, 393–400.

Stade, K., Ford, C. S., Guthrie, C., and Weis, K. (1997). Exportin 1 (Crm1p) is an essential nuclear export factor. Cell *90*, 1041–1050.

Seewald, M. J., Kraemer, A., Farkasovsky, M., Korner, C., Wittinghofer, A., and Vetter, I. R. (2003). Biochemical characterization of the Ran-RanBP1-RanGAP system: are RanBP proteins and the acidic tail of RanGAP required for the Ran-RanGAP GTPase reaction? Mol. Cell. Biol. *23*, 8124–8136.

Tange, Y., Hirata, A., and Niwa, O. (2002). An evolutionarily conserved fission yeast protein, Ned1, implicated in normal nuclear morphology and chromosome stability, interacts with Dis3, Pim1/RCC1 and an essential nucleoporin. J. Cell Sci. *115*, 4375–4385.

Thon, G., and Verhein-Hansen, J. (2000). Four chromo-domain proteins of *Schizosaccharomyces pombe* differentially repress transcription at various chromosomal locations. Genetics *155*, 551–568.

Volpe, T. A., Kidner, C., Hall, I. M., Teng, G., Grewal, S. I., and Martienssen, R. A. (2002). Regulation of heterochromatic silencing and histone H3 lysine-9 methylation by RNAi. Science *297*, 1833–1837.

Weis, K. (2003). Regulating access to the genome: nucleocytoplasmic transport throughout the cell cycle. Cell *112*, 441–451.

Welch, K., Franke, J., Kohler, M., and Macara, I. G. (1999). RanBP3 contains an unusual nuclear localization signal that is imported preferentially by Importin-α3. Mol. Cell. Biol. *19*, 8400–8411.